Joint Vortices, Eastward Propagating Eddies and Migratory Taylor Columns

DORON NOF

Department of Oceanography, The Florida State University, Tallahassee, FL 32306

(Manuscript received 15 November 1984, in final form 17 April 1985)

ABSTRACT

The behavior of an isolated pair of vortices consisting of two eddies situated on top of each other in a three-layer ocean is examined analytically. The amplitudes of both eddies are high and, consequently, the two eddies behave as one unit and migrate together in the ocean. For this reason, it is proposed to call the system *joint vortices*. The eddies are of equal or opposite sign; each vortex is situated in a different layer so that there are two active layers and one passive layer.

Attention is focused on the behavior of joint vortices on a sloping bottom in the deep ocean and on a β plane in the upper ocean. That is, we consider deep joint eddies situated on an inclined floor in the lowest two layers of a three-layer ocean and upper joint eddies in the upper two layers. Special attention is given to the cases where one of the vortices is a lens-like eddy. Approximate solutions for slope (or β) induced drifts in the east-west direction are obtained.

It is found that because of the high amplitudes and the resulting nonlinear coupling, the joint eddies have a mutual drift which is very different from the drift that each individual vortex would have. For example, *while each individual vortex translates to the west in the absence of a conjugate vortex, the combined vortices may drift steadily to the east.* This bizarre behavior stems from the presence of a "planetary lift" which is the oceanic equivalent of the side pressure force associated with the so-called *Magnus effect*. It is directed at 90° to the *left* of the drifting eddies.

Other results of interest are: (i) Under some conditions, the *westward drift* of joint eddies consisting of two cyclonic vortices is much faster than the long-wave speed. Such fast drifts contradict previously held contentions that the speed of cyclonic eddies cannot exceed the long wave speed. (ii) As it translates westward, an anticyclonic lens-like eddy can carry a Taylor column on top of it.

Possible application of this theory to various eddies in the ocean is discussed.

I. Introduction

a. Background

The dynamics of planetary vortices received much attention in recent years mainly because of the recognition that they play a major role in the transfer of energy, heat and nutrients (e.g., The Ring Group, 1981; Hogg and Stommel, 1985). This transfer is, at least partly, a result of the eddies' self-propulsion mechanisms, i.e., their ability to migrate without any external assistance. An important self-propulsion mechanism is believed to be a result of the variation of the Coriolis parameter with latitude. Consequently, there have been a large number of both numerical and analytical attempts to determine the influence of β on the eddy's behavior (e.g., Warren, 1967; Flierl, 1977; McWilliams and Flierl, 1979; Mied and Lindemann, 1979, 1982; Davey and Killworth, 1984; Killworth, 1983; Nof, 1981, 1983b; Shen, 1981; McWilliams *et al.*, 1981).

The attempts focused on various kinds of eddies, among them the so-called "Modons". These were introduced in the 1970s (Stern, 1975) as a means of simplifying the actual problem to a pair of adjacent vortices of equal strength and opposite sign. The direct applicability of the Modon to the ocean is somewhat limited mainly because of the lack of observations which clearly display the existence of adjacent eddies with opposite sign and equal strength. There is little doubt, however, that much has been learned from the introduction of the Modon mainly because of the various processes that can easily be examined with its aid.

In this paper we shall introduce a somewhat similar concept to the Modon. We shall look at the behavior of *a system consisting of two vortices (with high amplitudes) situated on top of each other in a three-layer ocean.* We term these eddies *joint vortices* because of the high amplitudes which "lock" the vortices to each other forcing them to translate together as one unit. In contrast to the Modon which includes two vortices of equal strength and opposite signs, the two eddies forming the new system are not necessarily of equal strength nor are they necessarily of opposite sign.

We shall consider three different systems of joint eddies. The first (system I) corresponds to deep ocean eddies situated on an inclined ocean floor; the second and third (systems II and III) correspond to upper ocean eddies subject to the influence of β. System II

© 1985 American Meteorological Society

corresponds to a lens situated above a cyclonic or anticyclonic vortex and system III corresponds to a lens situated underneath a cyclonic or anticyclonic vortex. For clarity, we shall first consider system I which, as it turns out, has the simplest solution. The solutions for systems II and III will be later derived on the basis of the—by then known—solution for system I.

b. *Method of solution*

The general method of solution for system I is similar to that described in Nof (1983a,b). That is, solutions for steadily drifting systems will be sought. We shall see that, although in the absence of a conjugate vortex each individual vortex translates steadily with the shallow water on its right side (i.e., "westward"), the joint vortices may translate with shallow water on their left (i.e., "eastward"). This unusual behavior is a result of the nonlinear coupling and the presence of a side pressure force which we shall call "planetary lift." It pushes the system to the left of its migratory direction. Much of the discussion is devoted to a detailed examination of the planetary lift and its relationship to the other forces acting on the system. An equivalent lift was found by Nof (1983b) to be of crucial importance for the migration of single isolated eddies. We shall see that this lift is also of crucial importance for the joint eddies and, for this reason, a thorough analysis of its properties is presented.

With the aid of the solution for system I, we shall proceed and present the solution for the somewhat more complicated situations (systems II and III). The general solution and balance of forces for these systems is quite similar to those of system I but the detailed solution is considerably more complicated. It will be shown that, in a similar fashion to deep ocean eddies, a lens with conjugate cyclonic vortex underneath can travel toward the east.

c. *Applications*

With the aid of the solutions for the three systems, we shall proceed and discuss the possible applicability of the model to various oceanic situations. For instance, we shall consider the possibility that the warm core rings north of the Kuroshio, which have been observed to move toward the northeast (rather than toward the west), can be represented by joint eddies. In addition, we shall examine the possibility that a special case of system III—a lens at middepth and a Taylor column on top—is relevant to the movement of intermediate eddies. In particular, we shall consider the so-called "Meddy" which is a lens containing water of Mediterranean origin "sandwiched" between two deep layers (e.g., see McDowell and Rossby, 1978).

d. *Structure*

Although an attempt has been made to make the present paper self contained, frequent references to Nof (1983a,b) are made. The reader who is interested in the detailed analysis is advised to look at Nof (1983a,b) before reading the present paper. On the other hand, readers who are interested only in the results may go directly to Table 1 (Section 8) and the summary.

This article is organized as follows: In Section 2 the model corresponding to system I is formulated and in Section 3 the general solution is given. Section 4 contains a detailed analysis of the solution for system I and Sections 5 and 6 contain the solutions for systems II and III. In Section 7 the behavior of migratory Taylor columns is discussed. The applications and limitations of the various models are discussed in Section 8 and Section 9 summarizes this work.

2. Formulation for system I (deep ocean eddies)

Consider the three-layer system shown in Fig. 1. Initially, our system consists of a lens-shaped eddy situated over a flat oceanic floor underneath a conjugate eddy (cyclonic or anticyclonic). The manner in which this system is set up is not important for

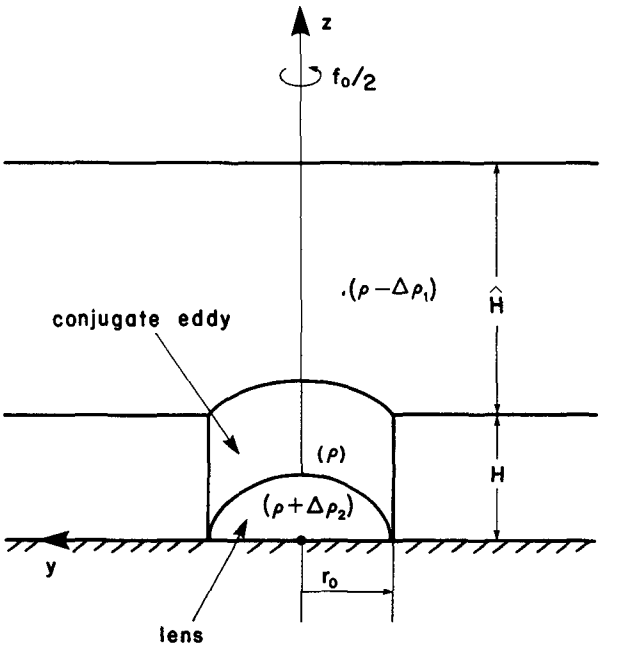

FIG. 1. Sketch of the initial basic state corresponding to system I. The joint vortices consist of two eddies situated on top of each other in a three layer ocean. Note that such a combination of eddies can be formed by the meandering of a system of currents shown in Fig. 2. The upper layer is infinitely deep (i.e., $\hat{H} \to \infty$) r_0 is the radius of eddies, and $\Delta\rho_1$ and $\Delta\rho_2$ are the density differences between the layers. Initially, the system is circular and stationary because the bottom is *flat*.

the present analysis but one can imagine that a system of two currents which became unstable could probably lead to such a combination (see Fig. 2). The strength of the conjugate eddy is not necessarily equal to that of the lens-shape eddy. The joint eddies and their surrounding waters are overlaid by a very deep upper layer which is taken to be at rest. Obviously, the joint eddies are initially stationary because there are no driving forces.

Suppose now that at some time (say, $t = 0$) a small uniform slope (s) is introduced to the floor. Immediately afterwards the joint eddies will start drifting because of (i) the gravitational force which tends to pull the blob toward the deep ocean and (ii) the slope-induced vortex force (i.e., the force similar to β). It is expected that, after an initial period of adjustment of $O(f_0)^{-1}$ (where f_0 is the Coriolis parameter), the eddies will migrate together as one unit because of the lens' high amplitude which traps the conjugate eddy. Namely, because of the large amplitudes, separation of the eddies from each other will introduce gross changes and large distortions in their structure. It is assumed that this cannot happen since the imposed perturbation (the bottom slope) is small so that the response should also be small. Note, however, that during the adjustment the eddies could move a distance of $O(g's/f_0^2) \sim O(Sl_1)$ [where $S = (sl_1/H)$, l_1 is the eddy's length scale and g' is the "reduced gravity" $(g\Delta\rho_1/\rho)$] relative to each other so that, in the final adjusted state, their centers do not necessarily coincide (Figs. 3 and 4).

Our aim is to find the joint eddies drift after the initial adjustment has been completed. For this purpose, consider the deviations of the hydrostatic pressures from those corresponding to a state of rest,

$$\Delta p_A = \xi_{2i}\Delta\rho_1 g \tag{2.1}$$

$$\Delta p_B = \xi_{2i}\Delta\rho_1 g + (h_1 + sy - z)g\Delta\rho_2 \tag{2.2}$$

$$\Delta p_C = \xi_{2e}\Delta\rho_1 g \tag{2.3}$$

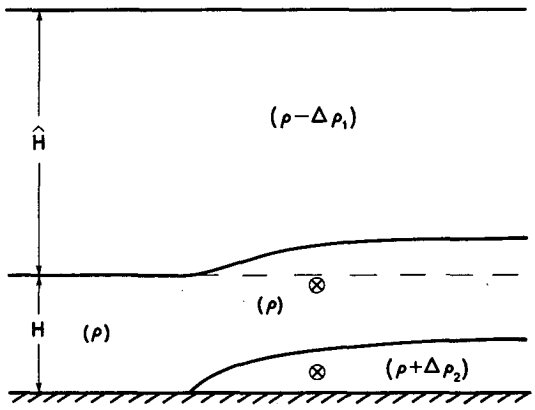

FIG. 2. Schematic diagram of two currents which, upon meandering, can produce the joint vortices under discussion.

where the points A, B and C correspond to the conjugate vortex, the lens, and the exterior fluid (Fig. 3). Here, ξ_2 is the upper interface vertical displacement (measured upward from the undisturbed depth), h_1 is the lens depth, g the gravitational acceleration, and $\Delta\rho_1$ and $\Delta\rho_2$ are the density differences between the intermediate layer and the upper and lower layers, respectively. The subscripts "i" and "e" indicate that the variable in question is associated with the "interior" (i.e., the conjugate eddy) and the "exterior" (i.e., the fluid surrounding the system). Our coordinate system is located at the center of the blob and is moving with the vortices at (the assumed steady) speed C; the y axis is pointing uphill, the x axis is oriented along the isobaths and the system rotates *uniformly* about the vertical axis (z).

With the aid of (2.1)–(2.3) the equations of momentum and continuity for the lens can be written in the form,

$$u_1\frac{\partial u_1}{\partial x} + v_1\frac{\partial u_1}{\partial y} - f_0 v_1 = -g'\frac{\partial \xi_2}{\partial x} - g''\frac{\partial h_1}{\partial x} \tag{2.4}$$

$$u_1\frac{\partial v_1}{\partial x} + v_1\frac{\partial v_1}{\partial y} + f_0(u_1 + C) = -g'\frac{\partial \xi_2}{\partial y} - g''s - g''\frac{\partial h_1}{\partial y} \tag{2.5}$$

$$\frac{\partial}{\partial x}(h_1u_1) + \frac{\partial}{\partial y}(h_1v_1) = 0 \tag{2.6}$$

where $g' = g\Delta\rho_1/\rho$, $g'' = g\Delta\rho_2/\rho$, and u_1 and v_1 are the horizontal two-dimensional velocity components [i.e., $u_1 = u_1(x, y)$, $v_1 = v_1(x, y)$] in the x and y direction. Note that h_1 is well defined *everywhere* because $h_1 \geq 0$ inside $\phi_1 = 0$ and $h_1 = 0$ outside $\phi_1 = 0$.

For the conjugate vortex situated above the lens the equations are,

$$u_{2i}\frac{\partial u_{2i}}{\partial x} + v_{2i}\frac{\partial u_{2i}}{\partial y} - f_0 v_{2i} = -g'\frac{\partial \xi_{2i}}{\partial x} \tag{2.7}$$

$$u_{2i}\frac{\partial v_{2i}}{\partial x} + v_{2i}\frac{\partial v_{2i}}{\partial y} + f_0(u_{2i} + C) = -g'\frac{\partial \xi_{2i}}{\partial y} \tag{2.8}$$

$$\frac{\partial}{\partial x}(h_{2i}u_{2i}) + \frac{\partial}{\partial y}(h_{2i}v_{2i}) = 0, \tag{2.9}$$

where h_{2i} is the conjugate vortex depth (see Fig. 3).

Similar equations hold for the fluid surrounding the vortices (i.e., the exterior) but, we shall see later that, it is more convenient to use the potential vorticity and Bernoulli integral,

$$\frac{\partial v_{2e}}{\partial x} - \frac{\partial u_{2e}}{\partial y} + f_0 = h_{2e}K_2(\psi_{2e}) \tag{2.10}$$

$$\frac{1}{2}(u_{2e}^2 + v_{2e}^2) + g'\xi_{2e} + f_0 Cy = G_2(\psi_{2e}) \tag{2.11}$$

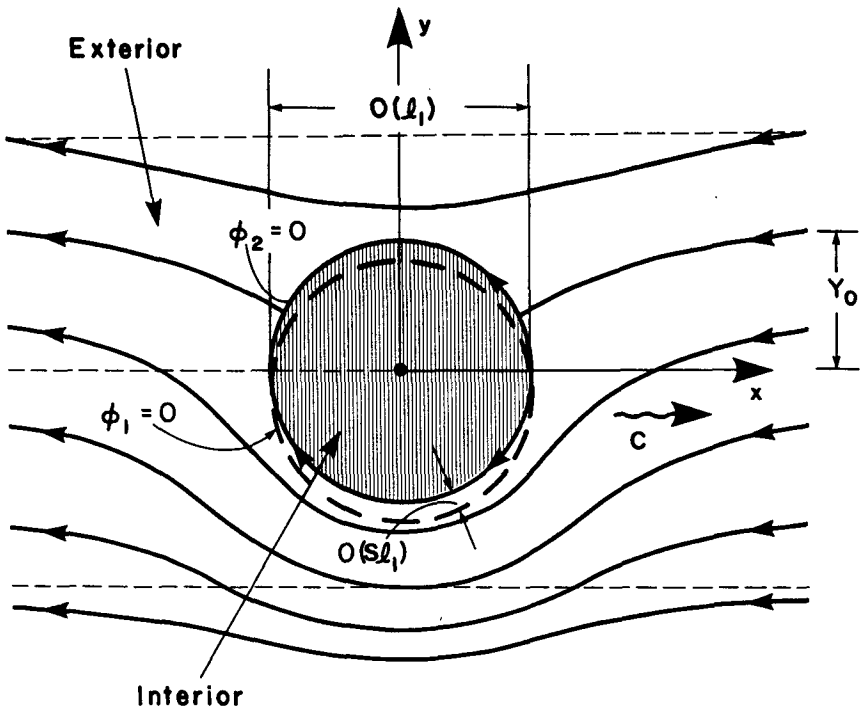

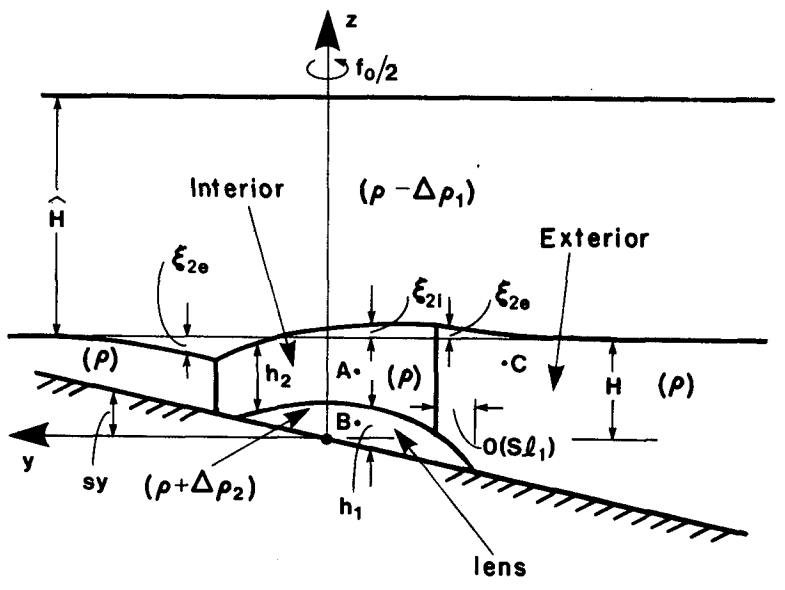

FIG. 3. Schematic diagram of the model for system I. The eddy structure under discussion results from a slope that was introduced to the system shown in Fig. 1. The "wiggly" arrow indicates migration; dashed lines denote the isobaths. The interface displacement ξ_2 is measured upward from the undisturbed depth; the vortex above the lens is referred to as the "interior" (denoted with the subscript "i") whereas the region surrounding the system is termed the "exterior" (denoted with the subscript "e"). Note that the centers of the two vortices do not necessarily coincide because, during the adjustment which followed the introduction of the slope, the eddies could move a distance of $O(Sl_1)$ relative to each other. It will become clear later that this relative movement does not enter the first-order approximations.

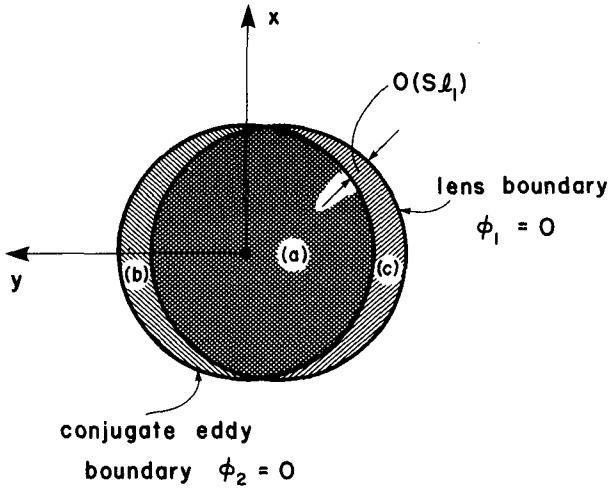

FIG. 4. A detailed view of the eddies' projection on the x, y plane. The curves $\phi_1 = 0$ and $\phi_2 = 0$ correspond to the lens and conjugated eddy boundaries, respectively. They are not necessarily circular but their departures from a circular geometry is not more than $\sim O(Sr_0)$. The symbols (a), (b) and (c) denote the mutual projection of the eddies, the projection of the strip occupied by the conjugate eddy alone and the projection of the strip occupied by the lens alone, respectively.

where $K_2 = dG_2/d\psi_{2e}$ and the stream function ψ_{2e} is defined by

$$\frac{\partial \psi_{2e}}{\partial x} = v_{2e}h_{2e}; \quad \frac{\partial \psi_{2e}}{\partial y} = -u_{2e}h_{2e}. \tag{2.12}$$

Note that (2.10) is the steady potential vorticity equation and that the dependence of $K_2(\psi)$ on $G_2(\psi)$ was first recognized by Charney (1955). The functions $K_2(\psi_{2e})$, $G_2(\psi_{2e})$ are found from the upstream conditions,

$$\begin{aligned} u_{2e} &= -C, & x &\to \infty \\ v_{2e} &= 0, & x &\to \infty \\ \psi_{2e} &= CH(y - Y_0), & x &\to \infty \\ h_{2e} &= H - sy, & x &\to \infty \end{aligned}$$

to be,

$$K_2(\psi_{2e}) = f_0/(H^2 - 2\psi_{2e}s/C - 2HY_0s + Y_0^2s^2)^{1/2} \tag{2.13a}$$

$$G_2(\psi_{2e}) = \frac{1}{2}C^2 + f_0CH/s - f_0C(H^2/s^2 - 2\psi_{2e}/Cs - 2HY_0/s + Y_0^2)^{1/2} \tag{2.13b}$$

where, for convenience, we have defined ψ_{2e} to be zero along the streamline separating the conjugate vortex from the environment [i.e., $\phi_2(x, y) = 0$] and Y_0 is the—yet unknown—latitude from which $\psi_{2e} = 0$ originates (Fig. 3). The reader who is not familiar with the determination of $K_2(\psi)$ and $G_2(\psi)$ from some known upstream conditions is again referred to Charney (1955) where a similar analysis is made.

Since friction is absent from our problem, pressure is the only mechanism which allows communication between the various regions. Consequently, we have the following matching conditions along the free separating streamline:

$$\xi_{2i} = \xi_{2e}; \qquad \phi_2(x, y) = 0 \tag{2.14}$$

$$\psi_{2i} = \psi_{2e} = 0; \quad \phi_2(x, y) = 0. \tag{2.15}$$

Relation (2.14) reflects the continuity of pressure whereas (2.15) assures that the boundary is a streamline of both the vortex and the surrounding fluid. For convenience, we also define,

$$\psi_1 = 0 \quad \text{along} \quad \phi_1(x, y) = 0, \tag{2.16}$$

where

$$\frac{\partial \psi_1}{\partial y} = -u_1h_1; \quad \frac{\partial \psi_1}{\partial x} = v_1h_1.$$

3. General solution for system I

a. *Balance of integrated forces*

To obtain the solution, (2.5) and (2.8) are multiplied by h_1 and h_{2i} (respectively) and then integrated over their corresponding areas. This gives

$$\iint_{(a)+(c)} \left[\frac{\partial}{\partial x}(h_1u_1v_1) + \frac{\partial}{\partial y}(h_1v_1^2) - f_0\frac{\partial \psi_1}{\partial y} + f_0Ch_1\right]dxdy = -g' \iint_{(a)+(c)} h_1\frac{\partial \xi_2}{\partial y}\,dxdy - g'' \iint_{(a)+(c)} \left[sh_1 + \frac{1}{2}\frac{\partial}{\partial y}(h_1)^2\right]dxdy \tag{3.1a}$$

$$\iint_{(a)+(b)} \left[\frac{\partial}{\partial x}(h_{2i}u_{2i}v_{2i}) + \frac{\partial}{\partial y}(h_{2i}v_{2i}^2) - f_0\frac{\partial \psi_{2i}}{\partial y} + f_0Ch_{2i}\right]dxdy = -g' \iint_{(a)+(b)} h_{2i}\frac{\partial \xi_{2i}}{\partial y}, \tag{3.1b}$$

where the continuity equation has been used to express the nonlinear terms and we have introduced the stream function,

$$\frac{\partial \psi_{2i}}{\partial y} = -u_{2i}h_{2i}; \quad \frac{\partial \psi_{2i}}{\partial x} = v_{2i}h_{2i}. \tag{3.2}$$

The symbols (a), (b) and (c) denote the various regions as shown in Fig. 4.

Equations (3.1a) and (3.1b) can be simplified by, (i) using Stokes' theorem to express the surface integrals (which include derivatives with respect to x and y) in terms of contour integrals, (ii) noting that $h = 0$ along $\phi_1 = 0$, and (iii) recalling that, since the edge is a streamline, $u_{2i}dy = v_{2i}dx$ along $\phi_2 = 0$. One ultimately finds,

$$f_0C \iint_{(a)+(c)} h_1 dxdy = -g' \iint_{(a)+(c)} h_1 \frac{\partial \xi_{2i}}{\partial y} dxdy - g''s \iint_{(a)+(c)} h_1 dxdy \quad (3.3a)$$

$$f_0C \iint_{(a)+(b)} h_{2i} dxdy = -g' \iint_{(a)+(b)} h_{2i} \frac{\partial \xi_{2i}}{\partial y} dxdy. \quad (3.3b)$$

Note that at this stage of the development, it is difficult to give a simple physical identification of all the terms in the equations. Some terms correspond to the Coriolis force associated with the migration, others correspond to the lens gravitational force, the vortex slope force and the pressure exerted on the vortices by the surrounding fluid. There are also some mixed terms and, for this reason, we shall give our physical interpretation later on after the structure of the equations is considerably simplified. We proceed now by adding (3.3a) and (3.3b) which, since $h_1 = 0$ outside $\phi_1 = 0$, gives

$$f_0C \iint_{(a)+(b)} (h_1 + h_{2i}) dxdy + f_0C \iint_{(c)} h_1 dxdy = -g' \iint_{(a)+(b)} (h_1 + h_{2i}) \frac{\partial \xi_{2i}}{\partial y} dxdy - g''s \iint_{(a)+(c)} h_1 dxdy - g' \iint_{(c)} h_1 \frac{\partial \xi_{2e}}{\partial y} dxdy.$$

This equation can be further simplified by using Stokes' theorem again which gives

$$f_0C \iint_{(a)+(b)} (h_1 + h_{2i}) dxdy + f_0C \iint_{(c)} h_1 dxdy = g'H \oint_{(a)+(b)} \xi_{2i} dx + \frac{g'}{2} \oint_{(a)+(b)} \xi_{2i}^2 dx + g's \iint_{(a)+(b)} y \frac{\partial \xi_{2i}}{\partial y} dxdy - g''s \iint_{(a)+(c)} h_1 dxdy - g' \iint_{(c)} h_1 \frac{\partial \xi_{2e}}{\partial y} dxdy. \quad (3.4)$$

Using the matching conditions (2.14) and (2.15), and the Bernoulli integral (2.11) and (2.13), Eq. (3.4) can be written as

$$f_0C \iint_{(a)+(b)} (H + \xi_{2i} - sy) dxdy + \iint_{(c)} \left(f_0C + g' \frac{\partial \xi_{2i}}{\partial y} \right) h_1 dxdy + g''s \iint_{(a)+(c)} h_1 dxdy + g's \iint_{(a)+(b)} \xi_{2i} dxdy = \oint_{(a)+(b)} \left[\frac{C^2}{2} + f_0C(Y_0 - y) - \frac{1}{2}(u_{2e}^2 + v_{2e}^2) \right] (H - sy) dx + \frac{1}{2g'} \oint_{(a)+(b)} \left[\frac{C^2}{2} + f_0C(Y_0 - y) - \frac{1}{2}(u_{2e}^2 + v_{2e}^2) \right]^2 dx. \quad (3.5)$$

Note that, so far, no approximations have been made so that (3.5) corresponds to an *exact balance of forces in the* y *direction.*

b. Perturbation analysis

To simplify the structure of (3.5), the following nondimensional scaled variables are introduced,

$$x^* = x/l_1; \quad y^* = y/l_1; \quad u_1^* = u_1/R_{01}f_0l_1;$$
$$v_1^* = v_1/R_{01}f_0l_1 \quad R_d = (g'H)^{1/2}/f_0;$$
$$C^* = C/R_{01}f_0l_1; \quad Y_0^* = Y_0/l_1$$
$$u_{2e}^* = u_{2e}/R_0f_0l_1; \quad v_{2e}^* = v_{2e}/R_{01}f_0l_1;$$
$$h_1^* = h_1/H \quad h_{2i}^* = h_{2i}/H; \quad \xi_{2i}^* = \xi_{2i}/H;$$
$$\xi_{2e}^* = \xi_{2e}/H; \quad S = \frac{sl_1}{H}. \quad (3.6)$$

Here, l_1 is the lens size, R_d the internal deformation radius, and R_{01} is the lens' Rossby number. For deep ocean eddies we take, $l_1 \sim 30$ km, $R_d \sim 10$ km, $s \sim 10^{-3}$, $f_0 \sim 10^{-4}$ s^{-1}, $R_{01} \sim 0.3$, $u_1 \sim$ O(10) cm s^{-1}, $H \sim 500$ m, $\Delta\rho/\rho \sim 10^{-4}$, and $g's/f_0 \sim$ O(1) cm s^{-1}. In view of these, we shall focus our attention on the following scales,

$$(x^*, y^*) \sim \text{O}(1); \quad (u_1^*, v_1^*, u_{2i}^*, v_{2i}^*) \sim \text{O}(1)$$
$$S \ll 1; \quad (C^*, u_{2e}^*, v_{2e}^*) \sim \text{O}(S); \quad Y_0^* \sim \text{O}(1)$$
$$\xi_{2i}^* \sim \text{O}(1); \quad \xi_{2e}^* \sim \text{O}(S);$$
$$(h_1^*, h_2^*) \sim \text{O}(1); \quad (l_1/R_d) \gtrsim 1$$
$$R_{01} \lesssim 1; \quad R_{01}(l_1/R_d)^2 \sim \text{O}(1). \quad (3.6a)$$

In terms of the variables defined by (3.6), the governing equation (3.5) is,

$$C^* \iint_{(a^*+b^*)} dx^*dy^* + \left[C^* + \frac{1}{R_{01}}\left(\frac{R_d}{l_1}\right)^2 S\right] \iint_{(a^*+b^*)} \xi_{2i}^* dx^*dy^* - SC^* \iint_{(a^*+c^*)} y^*dx^*dy^*$$
$$+ S \iint_{(c^*)} \left[C^* + \frac{1}{R_{01}}\left(\frac{R_d}{l_1}\right)^2 \partial\xi_{2i}^*/\partial y^*\right] h_{1c}^* dx_c^* dy^*$$
$$+ \frac{g''}{g'}\left(\frac{1}{R_{01}}\right)\left(\frac{R_d}{l_1}\right)^2 S \iint_{(a^*+b^*)} h_1^* dx^*dy^* + \frac{g''}{g'}\left(\frac{1}{R_{01}}\right)\left(\frac{R_d}{l_1}\right)^2 S^2 \iint_{c^*} h_1^* dx_c^* dy^*$$
$$= \oint_{(a^*+b^*)} \left\{\frac{R_{01}}{2}(C^*)^2 + C^*(Y_0^* - y^*) - \frac{R_{01}}{2}[(u_{2e}^*)^2 + v_{2e}^*)^2]\right\}(1 - Sy^*)dx^*$$
$$+ \frac{R_{01}}{2} \oint_{(a^*+b^*)} \left\{\frac{R_{01}}{2}\left(\frac{l_1}{R_d}\right)(C^*)^2 + \left(\frac{l_1}{R_d}\right)C^*(Y_0^* - y) - \frac{R_{01}}{2}\left(\frac{l_1}{R_d}\right)[(u_{2e}^*)^2 + (v_{2e}^*)^2]\right\}^2 dx^* \quad (3.7)$$

where, in nondimensionalizing the second term on the left-hand side of (3.5) [which is the fourth term on the left-hand side of (3.7)], it has been taken into account that the integral is to be computed over a narrow strip near the lens' edge. That is, since the area of (c) is $\sim O(Sl_1^2)$ we have introduced the scales

$$h_{1c}^* = h_1/H \quad x_c^* = x/Sl_1$$

where the subscript "c" denotes association with region (c) (see Fig. 4).

It is further assumed that the dependent variables can be expanded in a power series, i.e.,

$$C^* = SC^{(1)} + S^2C^{(2)} + \cdots;$$
$$h_1^* = h_1^{(0)} + Sh_1^{(1)} + \cdots;$$
$$h_{1c}^* = Sh_{1c}^{(1)} + S^2h_{1c}^{(2)} + \cdots;$$
$$\xi_{2i}^* = \xi_{2i}^{(0)} + S\xi_{2i}^{(1)} + \cdots;$$
$$u_{2e}^* = Su_{2e}^{(1)} + S^2u_{2e}^{(2)} + \cdots;$$
$$v_{2e}^* = Sv_{2e}^{(1)} + S^2v_{2e}^{(2)} + \cdots \quad (3.8)$$

$$\iint_{(a^*+b^*)} dx^*dy^* = \iint_{(a+b)^{(0)}} dx^*dy^* + S \iint_{(a+b)^{(1)}} dx^*dy^* + \cdots.$$

It is assumed, then, that the structure of the migrating joint vortices does not differ much from the circular and stationary structure that the joint vortices had on the *flat* floor before the slope was introduced. Note that (a* + b*), (a + b)$^{(0)}$ and (a + b)$^{(1)}$ correspond to the conjugate vortex nondimensional area, the area that the conjugate eddy would have on a flat bottom and the perturbed area (respectively).

Substitution of (3.8) into (3.7) and collecting terms of O(S) gives

$$\underbrace{SC^{(1)} \iint_{(a+b)^{(0)}} (1 + \xi_{2i}^{(0)})dx^*dy^*}_{\mathbf{A}}$$
$$\underbrace{+ \left(\frac{S}{R_{01}}\right)\left(\frac{R_d}{l_1}\right)^2 \iint_{(a+b)^{(0)}} \xi_{2i}^{(0)} dx^*dy^*}_{\mathbf{B}}$$
$$\underbrace{+ \frac{g''}{g'}\left(\frac{S}{R_{01}}\right)\left(\frac{R_d}{l_1}\right)^2 \iint_{(a+b)^{(0)}} h_1^{(0)} dx^*dy^*}_{\mathbf{C}}$$
$$\underbrace{+ O(S^2) = -SC^{(1)} \oint_{(a+b)^{(0)}} y^*dx + O(S^2)}_{\mathbf{D}} \quad (3.9)$$

It will become clear later that the terms **A**, **B**, **C**, and **D** are the integrated Coriolis force acting on the whole system (i.e., the lens and its conjugate vortex), the slope-induced vortex force, the gravitational force associated with the lens and the pressure force exerted on the eddy by the surrounding fluid, respectively. Simple manipulations show that Eq. (3.9) can be reduced to

$$\left[C^{(1)} + \left(\frac{R_d}{l_1}\right)^2\left(\frac{1}{R_{01}}\right)\right] \iint_{(a+b)^{(0)}} \xi_{2i}^{(0)} dx^*dy^*$$
$$= \frac{-g''}{g'R_{01}}\left(\frac{R_d}{l_1}\right)^2 \iint_{(a+b)^{(0)}} h_1^{(0)} dx^*dy^* + O(S) \quad (3.10)$$

which in dimensional form is

$$C \approx \frac{-g's \iint_\alpha \bar{\xi}_2 dxdy - g''s \iint_\alpha \bar{h}_1 dxdy}{f_0 \iint_\alpha \bar{\xi}_2 dxdy}. \quad (3.11)$$

Here, the bars indicate that the variable in question is associated with the basic state (i.e., $\bar{\xi}_2 = H\xi_{2i}^{(0)}$, $\bar{h}_1 = Hh_1^{(0)}$), and α denotes the dimensional area associated with the basic state.

Three general comments should be made with regard to (3.11). First, if the intermediate layer is removed (i.e., $H \to 0$ and $\xi_2 \to h_1 + sy$) then the migration speed reduces to

$$C \approx -(g' + g'')s/f_0 \tag{3.12}$$

which is identical to the result discussed by Nof (1983a) for deep ocean blobs, as should be the case. Second, if the blob is removed (i.e., $h_1 \to 0$ everywhere) then (3.11) reduces to

$$C \approx -g's/f_0 \tag{3.13}$$

which states that the speed of *all single deep ocean eddies embedded in a layer of infinite extent is independent of their depth, size and intensity.* Nof (1983a) has shown that this is the case for lens-like vortices but it has not been shown before that this is also the case for *any deep ocean eddy.* Third, when $\bar{\xi}_2 \to 0$ the perturbation scheme breaks down because terms which have been ignored as small are no longer negligible.

4. Analysis of system I

a. The detailed solution and its implications

We shall now determine the joint eddies drift with the aid of (3.11). To do so, it is necessary to specify the depths corresponding to the initial basic state and these depend, of course, on the velocity distribution and the potential vorticity of each eddy. It is possible to take solutions corresponding to known potential vorticity distributions (e.g., Csanady 1979, Flierl 1979). This is what most authors prefer to do but there are three variables to the problem (v, h, and the potential vorticity K) and it does not really make any difference which one of the three is specified. Specifying the velocity is the most convenient choice and we shall, therefore, adopt this specification for our model. Previous work (e.g., Nof 1983b) has shown that integrals similar to those present in (3.11) are very insensitive to variation in the specified velocity structure. Consequently, it is sufficient to take such velocity profiles which can be easily used in relation (3.11). In view of this, we shall consider eddies with linear velocity profiles for our initial calculations. For practical purposes it may, under certain conditions, be more desirable to use parabolic profiles and the results for such distributions are given in the Appendix.

We begin, then, by assuming,

$$\overline{v_{\theta 1}} = -\gamma_1 R_{01} f_0 r; \quad \gamma_1 = \pm 1, \quad R_{01} \geqslant 0 \tag{4.1}$$

$$\overline{v_{\theta 2}} = -\gamma_2 R_{02} f_0 r; \quad \gamma_2 = \pm 1, \quad R_{02} \geqslant 0 \tag{4.2}$$

where, for convenience, we have introduced polar coordinates (r, θ) and $\gamma_1 = +1, -1$ (and $\gamma_2 = +1, -1$) for anticyclonic and cyclonic eddies, respectively.

The momentum equations for the basic state are

$$\frac{\bar{v}_{\theta 1}^2}{r} + f_0 \bar{v}_{\theta 1} - g' \frac{d\bar{\xi}_2}{dr} = g'' \frac{d\bar{h}_1}{dr}$$

$$\frac{\bar{v}_{\theta 2}^2}{r} + f_0 \bar{v}_{\theta 2} = g' \frac{d\bar{\xi}_2}{dr} \tag{4.3}$$

Substituting (4.1) and (4.2) into (4.3) and solving for $\bar{\xi}_2$ and $\bar{h}_1$,

$$\bar{\xi}_2 = \hat{\xi}_2 + \frac{f_0^2 r^2}{2g'} \gamma_2 R_{02}(\gamma_2 R_{02} - 1) \tag{4.4}$$

$$\bar{h}_1 = \hat{h}_1 + \frac{f_0^2 r^2}{2g''} [\gamma_1 R_{01}(\gamma_1 R_{01} - 1) - \gamma_2 R_{02}(\gamma_2 R_{02} - 1)], \tag{4.5}$$

where $\hat{\xi}_2$ and $\hat{h}_1$ are the interface displacement and depth at the center [i.e., $\hat{\xi}_1 = \xi_1(0)$, $\hat{h}_1 = \bar{h}_1(0)$]. Relations (4.4) and (4.5) can now be used with (3.11) to get the desired translation rate,

$$C = -\frac{g's}{f_0}\left[1 + \frac{g''\hat{h}}{g'\hat{\xi}_2}\right]. \tag{4.6}$$

This is shown in Fig. 5. Note that in the absence of a conjugate vortex, each individual vortex would have translated in the negative x direction (i.e., "westward" with shallow water on the right hand side) as stated by (3.12) and (3.13). Bizzare as it may seem, once combined to form the united vortices, the system can have a positive translation. Such an "eastward" migration occurs whenever $\hat{\xi}_2$ is negative and its absolute value $|\hat{\xi}_2|$ is less than $g''\hat{h}_1/g'$. The causes of this peculiar behavior are related to an intricate balance of forces acting on the joint eddies. Its properties are discussed below.

b. General balance

Consider the following forces acting on the system:

1) Gravitational force: This force is the downhill component of the lens weight relative to its environment. It corresponds to the third term on the left hand side of (3.9) (i.e., term **C**).

2) Integrated Coriolis force: This force results from the fact that the joint vortices are translating. It is directed to the right of the moving system and corresponds to the first term on the left hand side of (3.9) (i.e., term **A**).

3) Sloping bottom force: This is the "vortex slope force" and is associated solely with the vortex above the lens. It is equivalent to the β-force associated with upper ocean eddies. Namely, it results from the fact that as a particle is circulating within the vortex, it

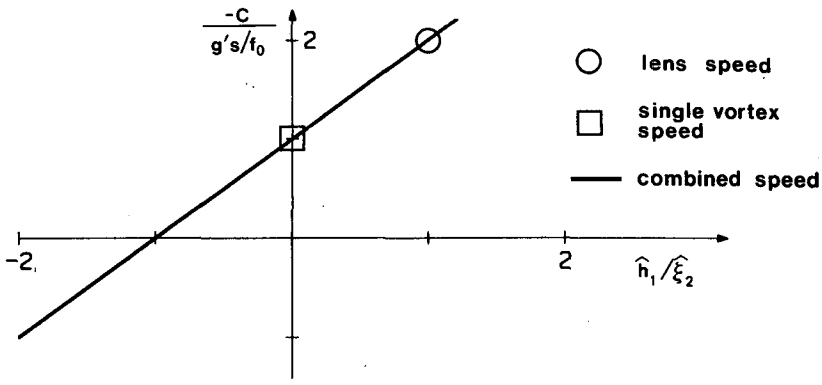

FIG. 5. The predicted migration speed for system I (with linear orbital speed) as a function of amplitude. Note that the migration speeds for both an individual lens and an individual vortex are directed toward the "west" (i.e., the eddies drift with shallow water on their right-hand side). Once combined, the joint vortices can drift either westward or eastward.

experiences high velocities in the shallow region and low in the deep region. This leads to a high Coriolis force on the shallow side and low on the deep side which, in turn, cause a net downhill force for anticyclonic eddies and an uphill force for cyclonic eddies. These forces correspond to the second term on the left hand side of equation (3.9) (i.e., term **B**).

4) "Planetary lift": Of the four forces acting on the united vortices, this is the most complicated one. The important contribution of side pressure forces to the dynamics of individual isolated eddies was already pointed out by Nof (1983b). In that article, it has been demonstrated that it is the mistaken neglect of this force which led Rossby (1948) to the erroneous conclusion that single cyclonic vortices move eastward on a β plane.

To examine the role that such a side pressure force plays in the problem at hand, we consider the Bernoulli integral,

$$\frac{1}{2}(u_{2e}^2 + v_{2e}^2) + \frac{p_{2e}}{\rho} + f_0 C y = B_{2e}(\psi_{2e}) \quad (4.7)$$

and its application to the innermost streamline of the surrounding fluid. Note that, as mentioned earlier, u_{2e}, $v_{2e} \sim O(C)$ because $l_1 \sim O(R_d)$ and the length scale of the flow outside the joint eddies is also R_d. Consequently, the ratio between the first and third terms on the left hand side of (3.14) is $O(C/f_0 l_1) \sim O(g's/f_0^2 l_1) \sim O(S)$. Hence, to first order, (4.7) can be approximated by

$$\frac{p_{2e}}{\rho} \approx B_{2e}(0) - f_0 C y \quad (4.8)$$

which states that, along $\psi_{2e} = 0$, the pressure decreases linearly with y (for positive C). This means that for $C > 0$ the pressure on the shallower side (large y) is smaller than the one on the deep side (small y) causing a side pressure force (i.e., a "planetary lift") in the positive y direction. For $C < 0$, the lift is directed in the opposite direction (i.e., downhill) showing that the *planetary lift is always directed to the left of the motion.*

Another way of looking at this "lift" is by examining the behavior of a quasi-geostrophic flow around a solid cylinder which is slowly translating in a barotropic ocean (Fig. 6). As the cylinder is moving in the positive x direction, fluid is displaced around and, subsequently, flows in the opposite direction. Since the drift is slow, the surrounding flow is close to being geostrophic (i.e., the Rossby number of the *exterior* flow C/fl is much smaller than unity) and the interface level on the right hand side is lower than that on the left. Consequently, a side pressure force is established (Fig. 6) and we can again apply the Bernoulli integral to show that this force is the lift given by (4.8).

Finally, it is instructive to examine the relationship between the planetary lift and the lift associated with the so-called "Magnus effect." For this purpose we re-consider the solid cylinder translating in a barotropic fluid. It is recalled that the Magnus side force is associated with the case where there is no Coriolis force, but there is some circulation around the cylinder (e.g., see Batchelor, 1967). The source of this circulation is not important for the present discussion but it can be thought of as being an indirect result of rotating the cylinder.

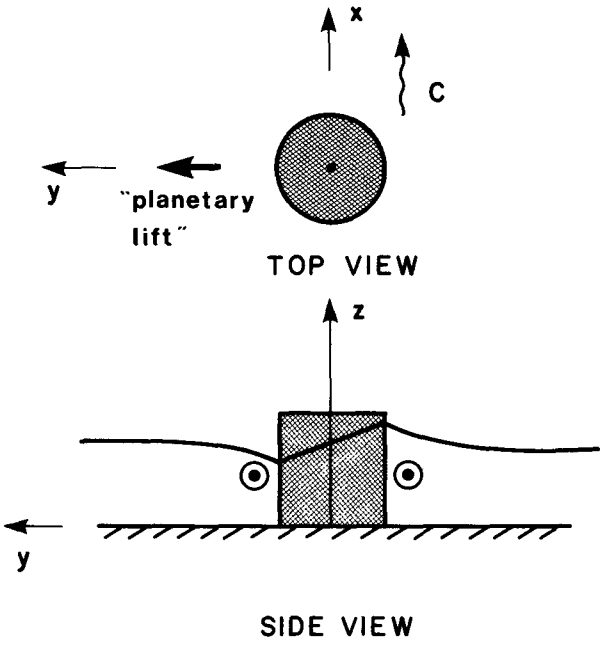

FIG. 6. Schematic diagram of the pressure side force ("planetary lift") exerted on a solid cylinder which slowly drifts in a barotropic ocean. As the cylinder is drifting, it displaces fluid to its sides. Since this displaced fluid is expected to be in a quasi-geostropic balance, the fluid on the right-hand side is higher than that on the left-hand side. Consequently, a force in the positive y direction is generated.

Under such conditions the velocities are low on one side of the cylinder and high on the other (e.g., see Batchelor, 1967, p. 425). This causes low pressure in the region where the velocities are high and high pressure in the region where the velocities are low because, in the absence of the Coriolis parameter, the quantity $\frac{1}{2}(u^2 + v^2) + p/\rho$ must be conserved along a streamline. It is, then, *the change in* $\frac{1}{2}(u^2 + v^2)$ *that is causing the Magnus side force whereas the change in* f_0Cy *is the one responsible for the planetary lift.* In other words, the Magnus side force is caused by the first term on the left hand side of (4.7) (which is usually negligible in the ocean) whereas the planetary lift is associated with the third term.

c. Implications

With the aid of the above information regarding the four active forces we return now to our discussion of the joint eddies' drift. It is easy to show that whether the system drifts westward or eastward depends on the relative magnitude of the forces in question. Since some of these forces depend on the system's internal structure and the others depend only on the depth around the edge, it is impossible to intuitively guess the direction at which a given system will migrate. All the possible combinations are shown in Fig. 7 which illustrates that an "eastward" propagation is certainly possible.

5. Joint upper ocean eddies with a light lens overlying a cyclonic or anticyclonic vortex (system II)

With the aid of the computations performed in the previous sections we shall now derive the migration speeds for joint upper ocean eddies consisting of a biconvex lens situated above a cyclonic or anticyclonic vortex (Fig. 8). The calculations are quite similar to those described earlier except that they are somewhat more involved. There are still only four forces acting on the system and these forces have properties similar to those described in Sections 3 and 4. However, the gravitational force associated with the blob is replaced by a β-induced force and the mathematical expressions are considerably more involved than those presented earlier.

As before, we begin by considering the deviations of the hydrostatic pressures (at points A, B, and C) from the pressure associated with a state of rest,

$$\left.\begin{aligned} \Delta p_A &= g\rho\eta_1 \\ \Delta p_B &= g\rho\eta_1 - g\xi_1\Delta\rho_1 \\ \Delta p_C &= g\rho\eta_{2e} \end{aligned}\right\} . \tag{5.1}$$

We take the lower layer to be motionless so that

$$\eta_1 = \frac{\Delta\rho_1}{\rho}\xi_1 + \frac{\Delta\rho_2}{\rho}\xi_{2i} \quad \text{and} \quad \eta_{2e} = \frac{\Delta\rho_2}{\rho}\xi_{2e}. \tag{5.2}$$

In view of these, the momentum equations (in the y direction) and the continuity equations can be written as,

$$u_1\frac{\partial v_1}{\partial x} + v_1\frac{\partial v_1}{\partial y} + (f_0 + \beta y)(u_1 + C) = -g'\frac{\partial\xi_1}{\partial y} - g''\frac{\partial\xi_{2i}}{\partial y} \tag{5.3}$$

$$u_{2i}\frac{\partial v_{2i}}{\partial x} + v_{2i}\frac{\partial v_{2i}}{\partial y} + (f_0 + \beta y)(u_{2i} + C) = -g''\frac{\partial\xi_{2i}}{\partial y} \tag{5.4}$$

$$\frac{\partial}{\partial x}(h_1u_1) + \frac{\partial}{\partial y}(h_1v_1) = 0; \qquad \frac{\partial}{\partial x}(h_{2i}u_{2i}) + \frac{\partial}{\partial y}(h_{2i}v_{2i}) = 0. \tag{5.5}$$

As in the deep ocean eddies case, it is convenient to use the potential vorticity equation and the Bernoulli integral for the exterior flow,

$$\frac{\partial v_{2e}}{\partial x} - \frac{\partial u_{2e}}{\partial y} + f_0 + \beta y = h_{2e}K_2(\psi_{2e}) \tag{5.6}$$

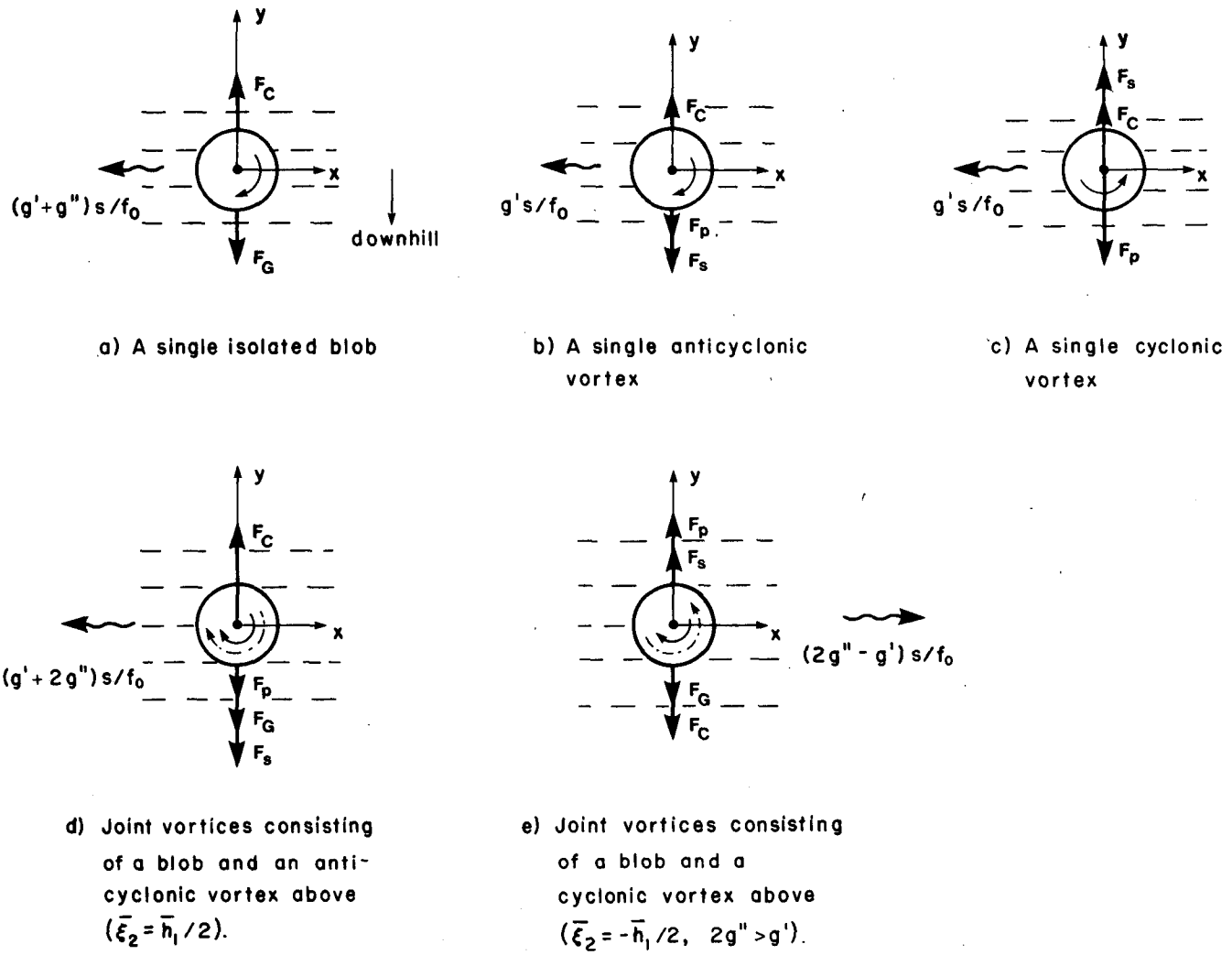

FIG. 7. The balance of integrated forces acting on the vortices. Thick solid arrows indicate the forces and, as before, "wiggly" arrows indicate direction of migration. Dashed lines denote the isobaths. In cases (a), (b) and (c) the eddies are not joint; namely, these are individual eddies which drift to the west. Their balance involves the lens' gravitational force F_G, the coriolis force F_C, the vortex slope force F_s and the side pressure force (planetary lift) F_p. In cases (b) and (c) the vortex slope force is pointing in different directions but its magnitude relative to the other forces imposes a westward drift. In cases (d) and (e) the eddies are joint and the forces are combined in such a way that both eastward and westward drifts are possible.

$$\frac{1}{2}(u_{2e}^2 + v_{2e}^2) + g''(h_{2e} - H_2) + (f_0 + \beta y/2)Cy = G_2(\psi_{2e}). \quad (5.7)$$

By considering the fact that the fluid is at rest at infinity (see Nof, 1983b), the functions $K_2(\psi_{2e})$ and $G_2(\psi_{2e})$ are found to be

$$K_2(\psi_{2e}) = \frac{f_0}{H_2} + \frac{\beta\psi_{2e}}{CH_2^2} + \frac{\beta Y_0}{H_2} \quad (5.8)$$

$$G_2(\psi_{2e}) = \frac{1}{2}C^2 + \left(f_0 + \frac{\beta\psi_{2e}}{2CH} + \frac{\beta Y_0}{2}\right)\left(\frac{\psi_{2e}}{H_2} + CY_0\right). \quad (5.9)$$

To obtain the solution we proceed, as previously, by taking the following steps. First, we multiply (4.3) and (4.4) by h_1 and h_{2i} (respectively) and then integrate each of the resulting equations over their corresponding areas using the continuity equation and Stokes' theorem to show that the integrals over the nonlinear terms vanish identically. Second, we express the terms involving the product $(f_0 + \beta y)uh$ as $-\partial[(f_0 + \beta y)\psi]/\partial y + \beta\psi$, choose the streamfunctions ψ_1 and ψ_2 to be zero along the edges (i.e., $\psi_1 = 0$ along $\phi_1 = 0$ and $\psi_2 = 0$ along $\phi_2 = 0$) and, using the Bernoulli integral, express the pressure in terms of the exterior flow. Third, we scale the equations using (3.6) with the small parameter S replaced by $\epsilon = \beta l_1/f_0$, and then expand in power series in ϵ to find,

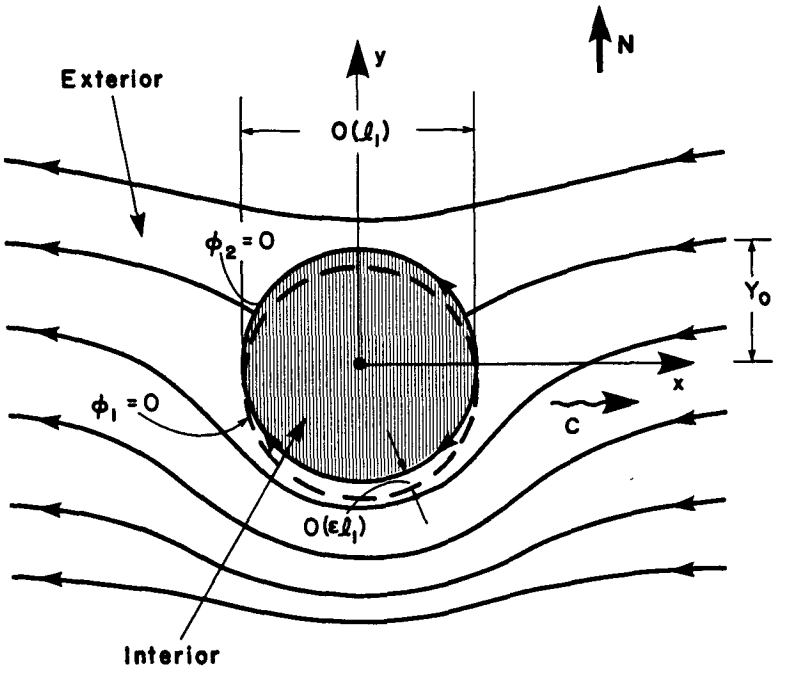

TOP VIEW

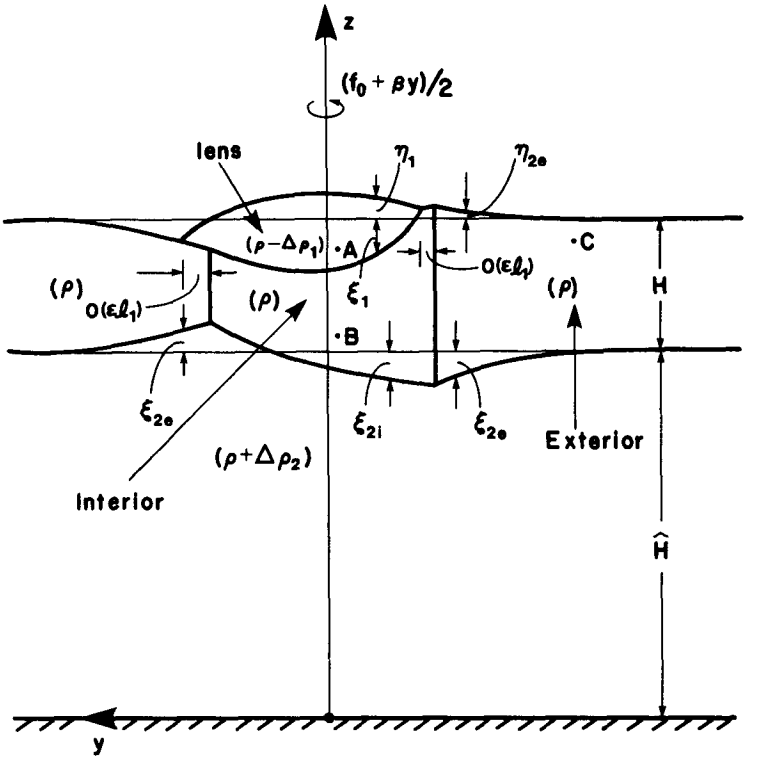

SIDE VIEW

FIG. 8. A sketch of upper ocean joint vortices with a lens on top of the conjugate eddy (system II). The interface displacements ξ_1, ξ_2 are measured downward from the undisturbed depths and the free surface displacements η_1, η_2 are measured upward. The lower layer is taken to be infinitely deep (i.e., $\hat{H} \to \infty$).

$$C^* = -\epsilon \iint_{(a+b)^{(0)}} [\psi_1^{(0)} + \psi_2^{(0)}]dx^*dy^* \Big/ \iint_{(a+b)^{(0)}} \xi_2^{(0)}dx^*dy^* + O(\epsilon^2) + \cdots \quad (5.10)$$

where $(a + b)^{(0)}$ is the area that the joint vortices would have on an f plane. Note that, with the exception of S, the scales of (3.6) and (3.6a) are also appropriate for upper ocean eddies and Gulf Stream rings because, for these features, $l_1 \sim 100$ km, $R_d \sim 40$ km, $\beta \sim 2 \times 10^{-11}$ m^{-1} s^{-1}, $f_0 \sim 10^{-4}$ s^{-1}, $R_{01} \sim 0.3$, u_{2i}, $u_1 \sim 1$ m s^{-1}, $H \sim 600$ m and $\Delta\rho_1/\rho \sim 10^{-3}$. For the purpose of computing the actual migration speed we shall again consider two velocity profiles—linear and parabolic. The results for the linear profile (4.1) and (4.2) are given below whereas those of the parabolic are presented in the Appendix.

The momentum equations for the basic state are similar, but not identical, to (4.3). They can be written in form

$$\bar{v}_{\theta 1}^2/r + f_0\bar{v}_{\theta 1} - g''d\bar{\xi}_2/dr = g'd\bar{\xi}_1/dr \quad (5.12)$$

$$\bar{v}_{\theta 2}^2/r + f_0\bar{v}_{\theta 2} = g''d\bar{\xi}_2/dr \quad (5.13)$$

which together with (4.1) give,

$$\xi_2 = \hat{\xi}_2\left\{1 + \frac{f_0^2r_0^2}{g''\hat{\xi}_2}\gamma_2R_{02}(\gamma_2R_{02} - 1)\left(\frac{r}{r_0}\right)^2\right\} \quad (5.14)$$

$$\xi_1 = \hat{\xi}_1\left\{1 + \frac{f_0^2r_0^2}{2g'\hat{\xi}_1}[\gamma_1R_{01}(\gamma_1R_{01} - 1) - \gamma_2R_{02}(\gamma_2R_{02} - 1)]\left(\frac{r}{r_0}\right)^2\right\} \quad (5.15)$$

and

$$r_0 = \left\{\frac{2g''\hat{\xi}_2}{\gamma_2R_{02}(1 - \gamma_2R_{02})}\right\}^{1/2} \Big/ f_0 \quad (5.16)$$

or

$$r_0 = \left\{\frac{2g'\hat{\xi}_1}{\gamma_1R_{01}(1 - \gamma_1R_{01}) - \gamma_2R_{02}(1 - \gamma_2R_{02})}\right\}^{1/2} \Big/ f_0 \quad (5.17)$$

where $\hat{\xi}_1$ and $\hat{\xi}_2$ correspond to the interface displacements at the center of the eddies ($r = 0$).

One also obtains, with the aid of (5.10),

$$C = \frac{\beta g''\hat{\xi}_2}{f_0^2}\{3[\gamma_1R_{01}\hat{\xi}_1/\hat{\xi}_2 + \gamma_2R_{02}(1 + H_2/\hat{\xi}_2 - \hat{\xi}_1/\hat{\xi}_2)] - 2[(\gamma_1R_{01} - \gamma_2R_{02})(\hat{\xi}_1/\hat{\xi}_2) + \gamma_2R_{02}]\} \times \{3\gamma_2R_{02}(\gamma_2R_{02} - 1)\}^{-1}. \quad (5.18)$$

For $\xi_1 \to 0$ (no lens) we recover Nof's (1983b) solution for an isolated vortex,

$$C = -\frac{\beta g''H_2(3 + \hat{\xi}_2/H_2)}{3f_0^2(1 - \gamma_2R_{02})} \quad (5.19)$$

and for $\xi_2 \to \xi_1$ and $H_2 \to 0$ (no conjugate vortex) we recover Nof's (1981) solution for an isolated lens,

$$C = -\beta r_0^2R_{01}/6. \quad (5.20)$$

The joint eddies migration speed (5.18) as a function of size is shown in Fig. 9, and as a function of amplitude and size is shown in Fig. 10. As in the bottom eddies case, eastward propagation is again possible. In this context, it is appropriate to point out that our eastward drift is not related to the Modon's eastward drift discussed by Mied and Lindemann (1982). The latter is associated with self advection and the speed that each vortex induces on its neighboring vortex. The fact that our eddies centers do not coincide (Fig. 8) may give the false impression that in our case self advection may also be possible. This is not the case because the distance between the eddies centers does not even enter our computation since each vortex is situated in a different layer.

6. Joint upper ocean eddies with an intermediate lens underneath a cyclonic or anticyclonic vortex (system III)

The combination of eddies appropriate to this case is shown in Fig. 11. At first glance this case appears to be very similar to the system considered previously (system II). We shall see, however, that the actual detailed solutions of the two systems are very different and that the case under present consideration is much more interesting than the previous one. It can be easily demonstrated, using the techniques described previously, that the general solution has a structure identical to that given by (5.10). Namely, in dimensional form, the drift is,

$$C \approx -\beta \iint_\alpha (\bar{\psi}_1 + \bar{\psi}_2)dxdy/f_0 \iint_\alpha \bar{\xi}_2dxdy \quad (6.1)$$

where, as before, α is the dimensional area that the joint vortices would have on an f plane.

Using the momentum equations

$$\bar{v}_{\theta 1}^2/r + f_0\bar{v}_{\theta 1} - g''\frac{d\bar{\xi}_2}{dr} = -g'\frac{d\bar{\xi}_1}{dr}$$

$$\bar{v}_{\theta 2}^2/r + f_0\bar{v}_{\theta 2} = g''d\bar{\xi}_2/dr,$$

and the linear velocity profile, (4.1) and (4.2), one finds the interface displacements, $\bar{\xi}_1$ and $\bar{\xi}_2$, to be,

$$\bar{\xi}_1 = \hat{\xi}_1\left\{1 - \frac{r^2f_0^2}{2g'\hat{\xi}_1}[\gamma_1R_{01}(\gamma_1R_{01} - 1) - \gamma_2R_{02}(\gamma_2R_{02} - 1)]\right\} \quad (6.2)$$

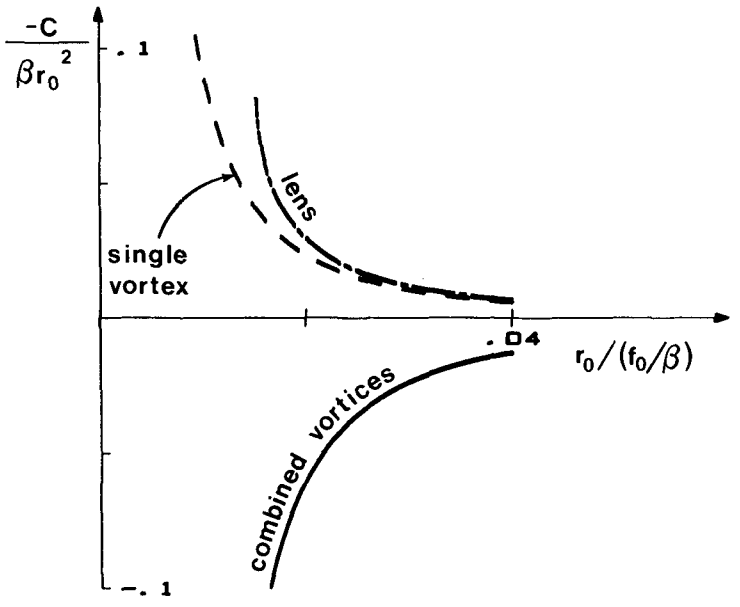

System II, $\Delta\rho_1/\Delta\rho_2 = 0.3$; $\hat{\xi}_1/\hat{\xi}_2 = -4$; $\hat{\xi}_2/\hat{H}_2 = -6$

$(g''\hat{\xi}_2)^{1/2}/f_0 = 6.5\,\text{km}$, $\beta = 2\times10^{-11}\,\text{m}^{-1}\,\text{sec}^{-1}$

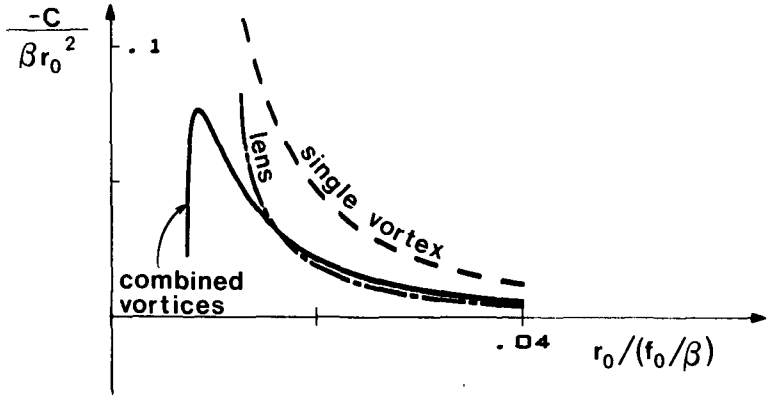

System II, $\Delta\rho_1/\Delta\rho_2 = 1$; $\hat{\xi}_1/\hat{\xi}_2 = -3$; $\hat{\xi}_2/H_2 = -1/6$

$(g''\hat{\xi}_2)^{1/2}/f_0 = 9\,\text{km}$, $\beta = 2\times10^{-11}\,\text{m}^{-1}\,\text{sec}^{-1}$

FIG. 9. The migration speed for system II (with a cyclonic conjugate vortex and a linear orbital velocity) as a function of the eddies' size. Note how different the joint eddies drift is from the drift that each individual vortex would have in the absence of its conjugate vortex. For a weak cyclonic vortex ($\bar{\psi}_2 < \bar{\psi}_1$) the system moves eastward (upper panel); for a strong cyclonic vortex (i.e., $\bar{\psi}_2 > \bar{\psi}_1$) the joint vortices drift westward (lower panel).

$$\bar{\xi}_2 = \hat{\xi}_2\left\{1 + \frac{r^2 f_0^2}{2g''\hat{\xi}_2}\,\gamma_2 R_{02}(\gamma_2 R_{02} - 1)\right\} \qquad (6.3)$$

$$C \approx \frac{\beta g'\hat{\xi}_2}{f_0^2}\left\{3[\gamma_1 R_{01}(H_1/\hat{\xi}_2 - \hat{\xi}_1/\hat{\xi}_2) + \gamma_2 R_{02}(1 + \hat{\xi}_1/\hat{\xi}_2)]\right.$$

The east–west drift is computed with the aid of (6.1), (6.2), (6.3) which give,

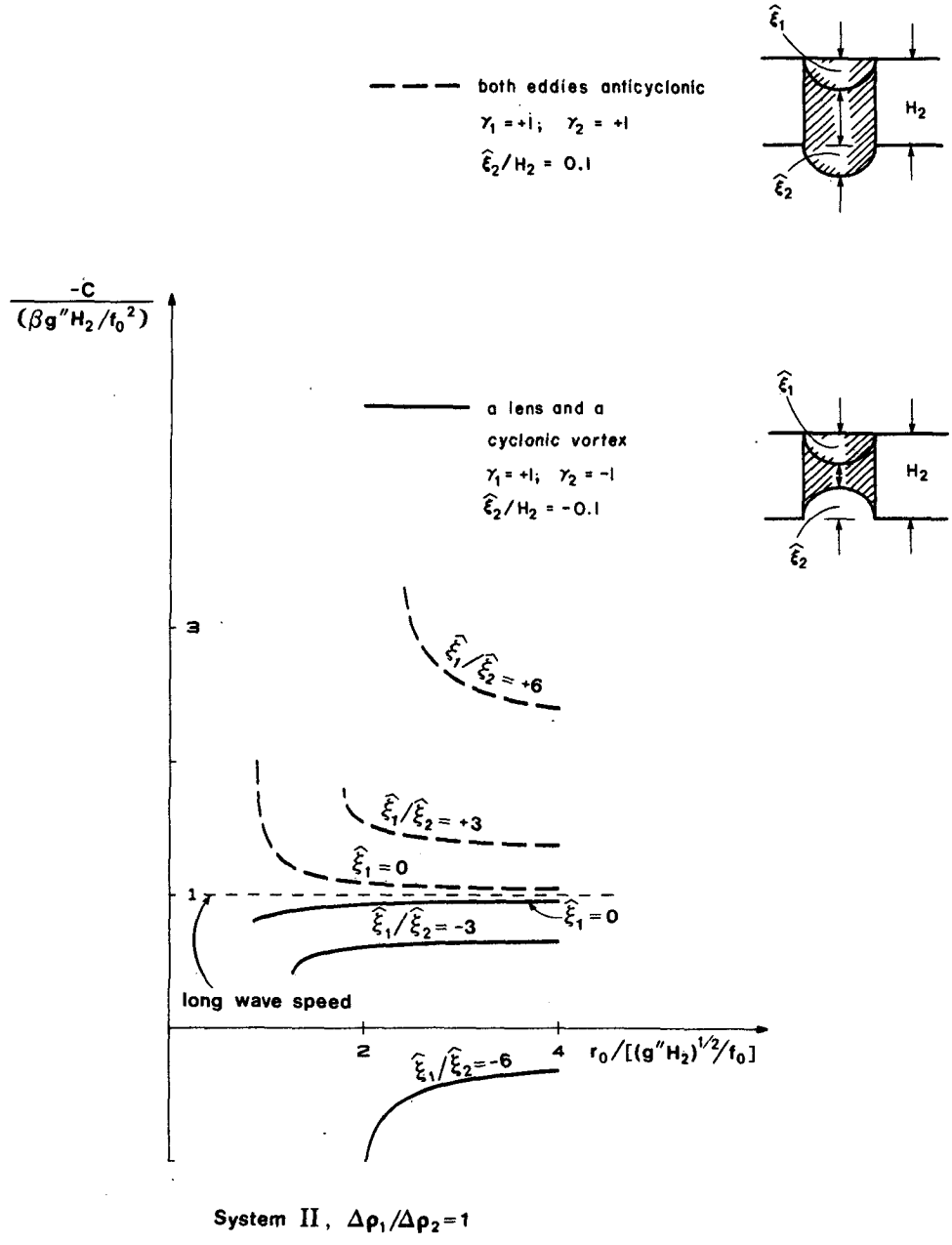

FIG. 10. The migration of system II (with a linear velocity profile) as a function of amplitude and size. Note that the long-wave speed is based on the environmental depth and the environmental stratification.

$$- 2\left[\gamma_2 R_{02} - \frac{\hat{\xi}_1}{\hat{\xi}_2}(\gamma_1 R_{01} - \gamma_2 R_{02})\right]\Big\} \times \{3\gamma_2 R_{02}(\gamma_2 R_{02} - 1)\}^{-1}. \quad (6.4)$$

Its dependence on the amplitude and size is shown in Fig. 12. Note that for $\xi_1 \to -\xi_2$ (no lens) we again recover Nof's (1983b) solution for isolated eddies.

7. Migratory Taylor columns

This is a special case of system III. It corresponds to the situation where the conjugate vortex is at rest relative to the biconvex lens. Namely, as the lens is drifting, it carries along a column of fluid above it. We can imagine that such a situation may arise whenever a lens is drifting into a shallow region where the upper layer depth (H_1) obeys

$$\frac{\hat{\xi}_1}{H_1} > \frac{C}{f_0 r_0} \quad (7.1)$$

which is the known necessary condition for the generation of Taylor columns above obstacles (see e.g., Taylor 1922, 1923; Hide, 1961; Jacobs, 1964;

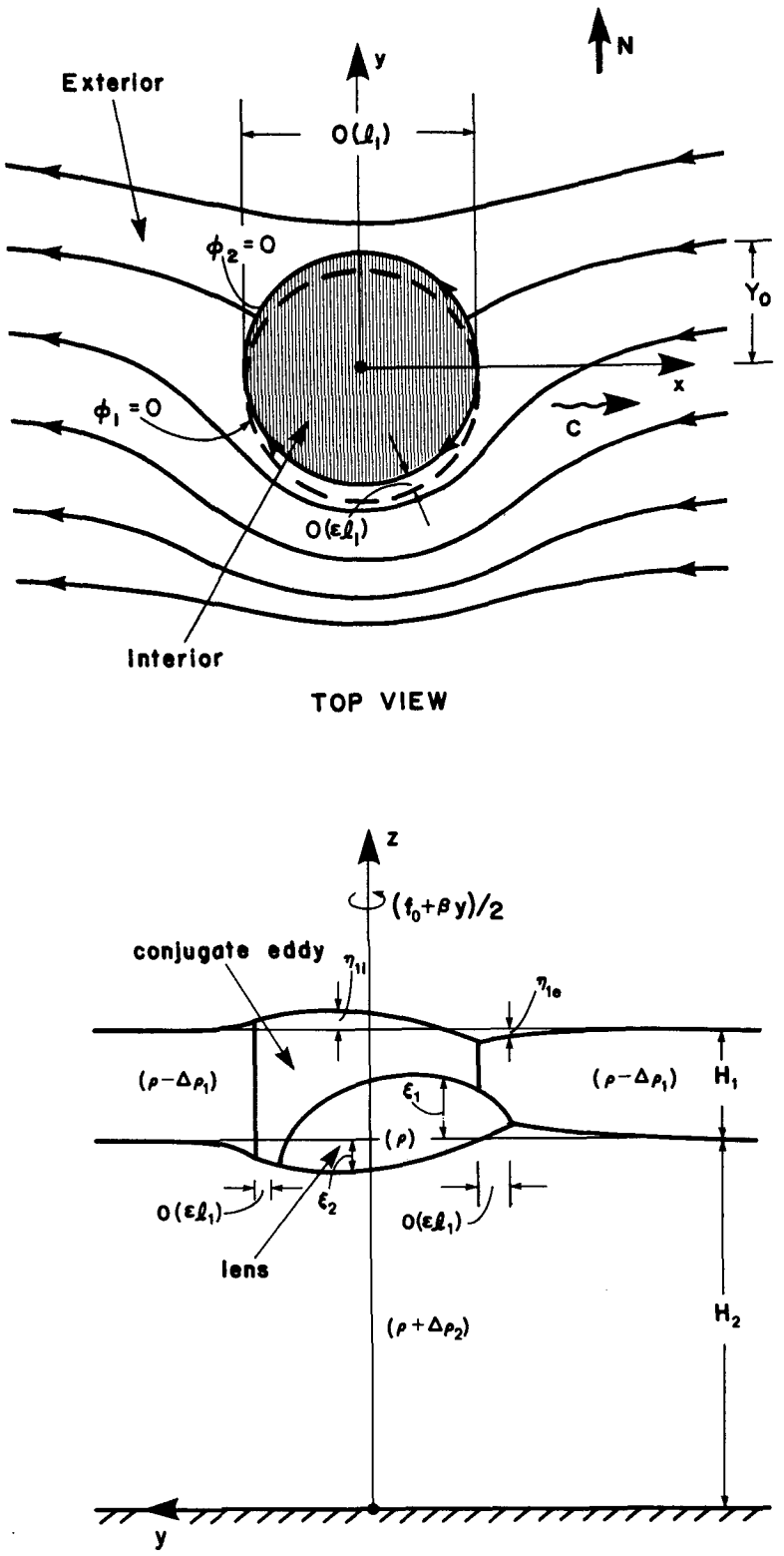

FIG. 11. Schematic diagram of upper joint eddies consisting of a lenslike eddy underneath a cyclonic or anticyclonic eddy (system III). The free surface displacements η_1 and the interface displacement ξ_1 are measured upward; the interface displacement ξ_2 is measured downward. The lower layer is infinitely deep ($H_2 \to \infty$).

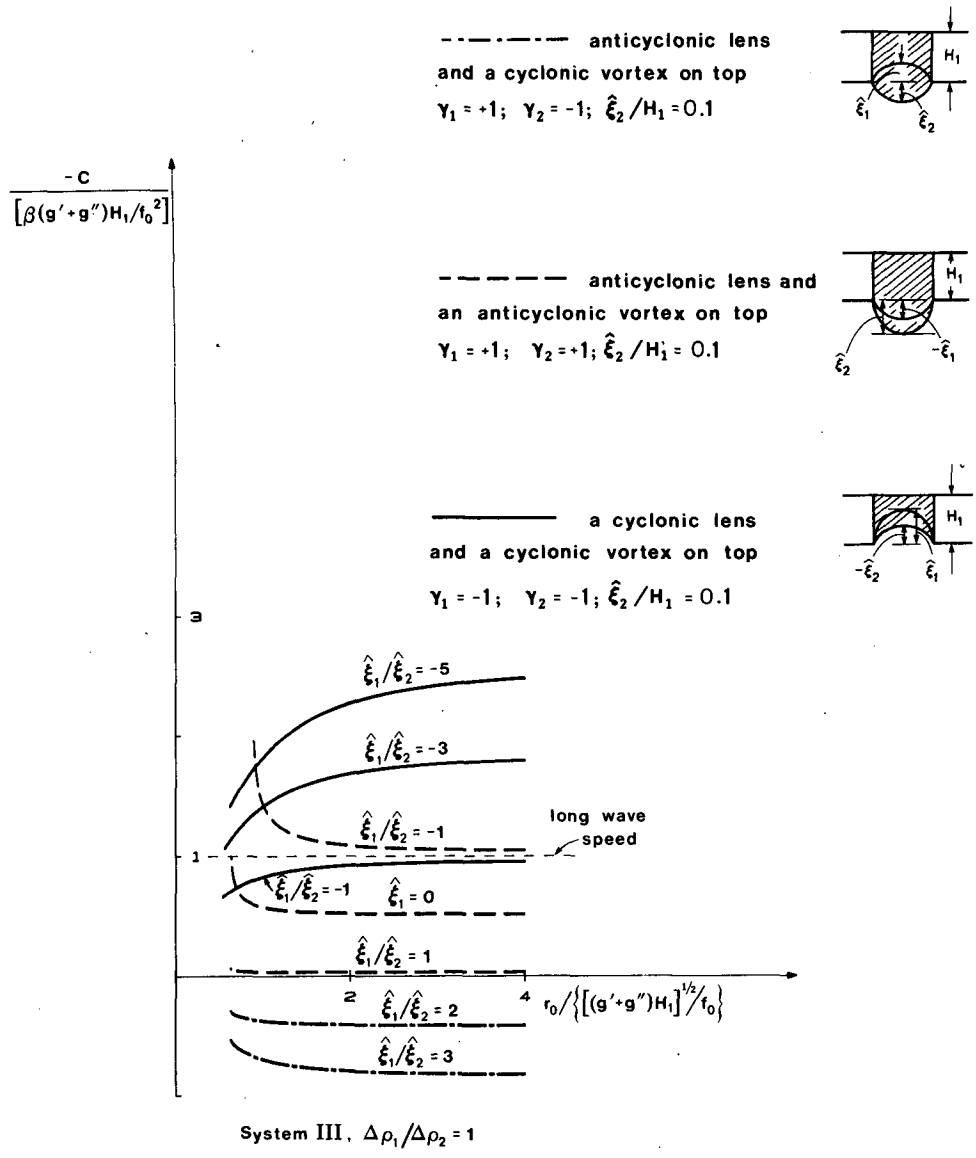

FIG. 12. The predicted migration speed for system III (with a linear velocity profile) as a function of size and amplitude. Note that (i) the system can drift eastward ($C > 0$), and (ii) joint eddies consisting of two cyclonic eddies can drift westward at a speed larger than the long wave speed.

Ingersoll, 1969; Hogg, 1973; Huppert, 1975; McCartney, 1975). The right-hand side of (7.1) is typically a few percent [because $C \sim$ O(1) cm s^{-1}, $f_0 \sim 10^{-4}$ s^{-1}, and $r_0 \sim$ O(10) km] whereas the left hand side is ~O(1) [because $\xi_1 \sim$ 100–500 m; $H_1 \sim$ 1000 m] so that the condition is easily satisfied. In fact, the condition $\xi_1/H_1 > C/f_0 r_0 \sim$ O(ϵ) is satisfied over the whole "blob" except a very narrow ~O(ϵr_0) ring near the edge.

The drift of the lens and column is found by taking the limit of the general drift (6.4) as $R_{01} \to 0$. Since the differences between the drifts of eddies with linear orbital speed and those with parabolic profile are minute, we shall focus our attention on the simpler group (i.e., eddies with linear speed). For these conditions we find from (6.4),

$$C_{lT} = -\frac{\beta g''(\hat{\xi}_1 + \hat{\xi}_2)}{3f_0^2(1 - R_{02})} \tag{7.2}$$

where the subscript "lT" indicates that the variable in question is associated with a lens and a Taylor column. This speed is slower than that of an identical isolated lens "sandwiched" between two infinitely deep layers,

$$C_l = -\frac{\beta g'(1 + \Delta\rho_1/\Delta\rho_2)(\hat{\xi}_1 + \hat{\xi}_2)}{3f_0^2(1 - R_{02})}, \tag{7.3}$$

where the subscript "l" denotes an association with a single isolated lens. The ratio between the two migration speeds is,

$$\frac{C_l}{C_{lT}} = 1 + \left(\frac{\Delta\rho_1}{\Delta\rho_2}\right). \tag{7.4}$$

Namely, when $\Delta\rho_1 = \Delta\rho_2$ the column and lens drift at half the speed of a single lens sandwiched between two infinitely deep layers.

Two comments should be made with regard to (7.4). First, it should be pointed out that of the three systems considered in this study (I, II and III) only the case described above corresponds to a Taylor column translating steadily to the west (or east). This does not mean that a heavy blob on a sloping floor (system I) cannot have a Taylor column above it nor does it imply that a light lens cannot have a column under it (system II). It merely indicates that if a lens produces a Taylor column in one of these latter cases, then it will move unsteadily in a direction different from the west (and east). Second, it is important to realize that the case corresponding to a mid-depth lens with a Taylor column on top may be relevant to various mesoscale vortices such as the so-called "Meddy" (see e.g., Nof, 1982). In this case, the ratio between the actual lens depth and the actual upper layer depth is ~0.5 so that a Taylor column may well be present on top of the lens. If this is indeed the case then the Meddy's β-induced speed is about half the speed predicted by Nof (1982).

8. Discussion

Our results for systems I, II and III are summarized in Table 1. It should be noted that there are upper and lower bounds on the Rossby numbers (R_{01}, R_{02}) that can be used with (4.4)–(4.6), (5.18) and (6.4) (see Fig. 13). These bounds result from, (i) the fact that the negative relative vorticity $1/r/d(r\bar{v}_\theta)/dr$ must be smaller than f_0 so that the eddies are inertially stable, and (ii) the conditions that $h_1 \geqslant 0$ and $h_2 \leqslant 0$ everywhere.

a. Applications

Before discussing any of our applications, it should be mentioned that the discussion in this subsection is largely conjectural because of the limited observational information that is available. A detailed application of our model requires a substantial amount of information on much of the water column (top to bottom) and the existing literature cannot provide it. With this point in mind we now turn to some specific examples. The first application which we shall discuss is that of the joint eddies shown by configuration 3 (Table 1) to the warm-core rings found north of the Kuroshio. The warm-core rings found in the region immediately to the east of Japan behave in a rather peculiar fashion. Instead of migrating westward as most warm rings do, they migrate northward and then toward the northeast (e.g., see Kitano, 1974, 1975; Ichye, 1955; Tomasada, 1978). Several sets of observations have confirmed this despite the fact that the mean flow in which the eddies are embedded has been traditionally viewed as a southwestward flowing current (e.g., Kawai, 1972; Cheney, 1977).

Our suggestion is, then, that this eastward movement could perhaps be a result of a weak cyclonic vortex situated underneath the warm-core rings. Unfortunately, the lack of deep sections across the rings does not allow any detailed quantitative comparison between the model and the observations. Most of the observations in the area in question are so shallow (<800 m) that we cannot even say whether there exists a conjugate cyclonic eddy. It should be pointed out, however, that for $\xi_2^{(0)} \sim O(1)$ the predicted migration speed is O(1 cm s^{-1}) which is of the same order as the observed drifts.

The second application which we shall consider is that of configuration 8 (Table 1) to cold-core Gulf Stream rings. These cold-core rings are known to trap and carry slope water as they migrate. A two-layer model (e.g., Nof, 1983b) cannot explain the trapping because the slope water which is carried along is usually found below the thermocline (e.g., The Ring Group, 1981). The three-layer model, on the other hand, resolves this because it allows for the slope water to be represented by the lens. Several observations suggest that such a structure may, in fact, exist. For example, the 10 and 11°C isotherms shown in Fig. 1 of Lai and Richardson (1977) can be thought of as the lower and upper boundaries of a converging meniscus lens.

The joint eddies concept corresponding to configuration 8 has an additional appealing aspect; the presence of a converging meniscus lens under the cold-ring allows for migration speeds higher than the long-wave speed. Two-layer models for isolated eddies (e.g., Nof, 1983b) consistently predict migration speeds which are too low (~2 cm s^{-1}) compared to the actual drift (~5 cm s^{-1}). Adding a lens underneath the ring can increase the predicted speed from ~2 to ~4 cm s^{-1}.

A third application which comes to mind is that of eastward propagating joint eddies consisting of a weak cyclonic ring with an anticyclonic vortex underneath (configuration 5, Table 1). This system may be relevant to some unusual cold-core Gulf Stream rings because on some occasions cold-rings were observed to move toward the northeast (e.g., Richardson *et al.*, 1977) even though there are indications that the mean flow is directed toward the west or southwest. A fourth application of the theory was already discussed in the previous section. It is related to the idea that Taylor columns can form above isolated lenses so that a system of a biconvex lens

TABLE 1. The drift of joint eddies.

	Configuration	Description	Direction of migration	Migration speed
System I, joint topographic eddies consisting of a lens underneath a cyclonic or anticyclonic vortex. The eddies are overlayed by an infinitely deep layer.	① 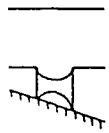	Plano-convex lens underneath a cyclonic vortex	"Eastward" when cyclonic vortex is weak[a] and "westward" when cyclonic vortex is strong	Eastward speed is unbounded[b] westward speed is $O(g's/f_0)$
	② 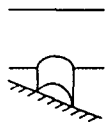	Plano-convex lens underneath an anticyclonic vortex	"Westward"	Unbounded
System II, joint upper ocean eddies consisting of a lens on top of a cyclonic or anticyclonic vortex. The vortices overlie an infinitely deep layer.	③ 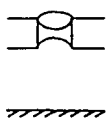	Biconvex lens on top of a cyclonic vortex	Eastward when cyclonic vortex is weak and westward when cyclonic vortex is strong	Eastward speed is unbounded, westward speed is slower than the long wave speed[c]
	④ 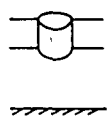	Biconvex lens on top of an anticyclonic vortex	Westward	Faster than the long wave speed
System III, joint upper ocean eddies consisting of a lens underneath a cyclonic or anticyclonic vortex	⑤ 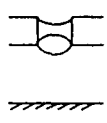	Biconvex lens underneath a cyclonic eddy	Eastward when cyclonic vortex is strong and westward when cyclonic vortex is weak	Eastward speed is unbounded, westward is less than the long wave speed
	⑥ 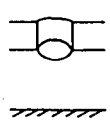	Biconvex lens underneath an anticyclonic eddy	Westward	Slower or faster than the long wave speed
	⑦ 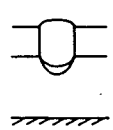	Converging meniscus lens underneath an anticyclonic vortex	Westward	Slower or faster than the long wave speed
	⑧ 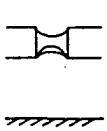	Converging meniscus lens underneath a cyclonic vortex	Westward	Unbounded
	⑨ 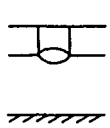	Biconvex lens with a resting Taylor column on top	Westward	Slower than the long wave speed and slower than the lens migration speed

[a] Hereafter, "weak" and "strong" indicate intensity relative to the lens.

[b] The term "unbounded" is used in the sense that the speed is not limited to the order of the long wave speed. It is, actually, bounded for two reasons. First, our perturbation scheme breaks down whenever the drift becomes comparable to the swirl speed. Secondly, it cannot grow beyond the values for which h_1; h_2 become zero and the values which cause a negative relative vorticity larger than f_0.

[c] The long wave speed is defined on the basis of the environmental undisturbed depth and the environmental stratification.

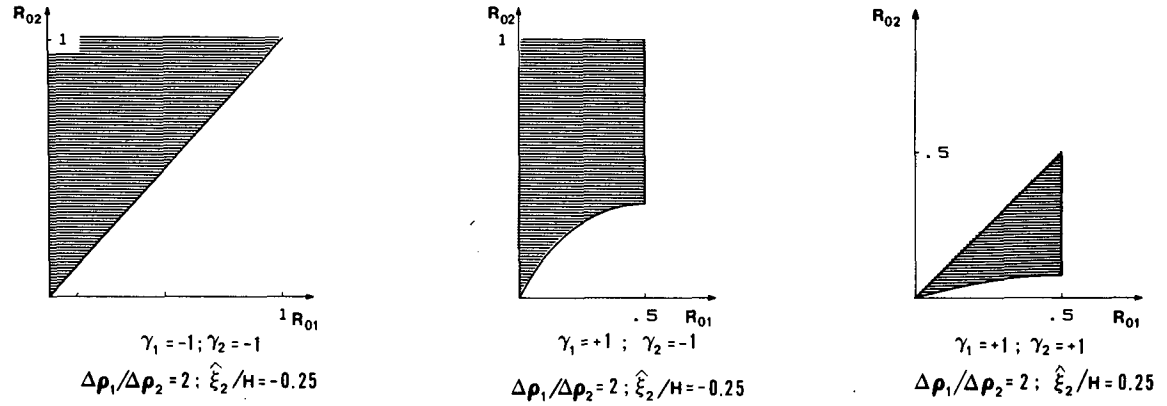

System I, linear velocity profile

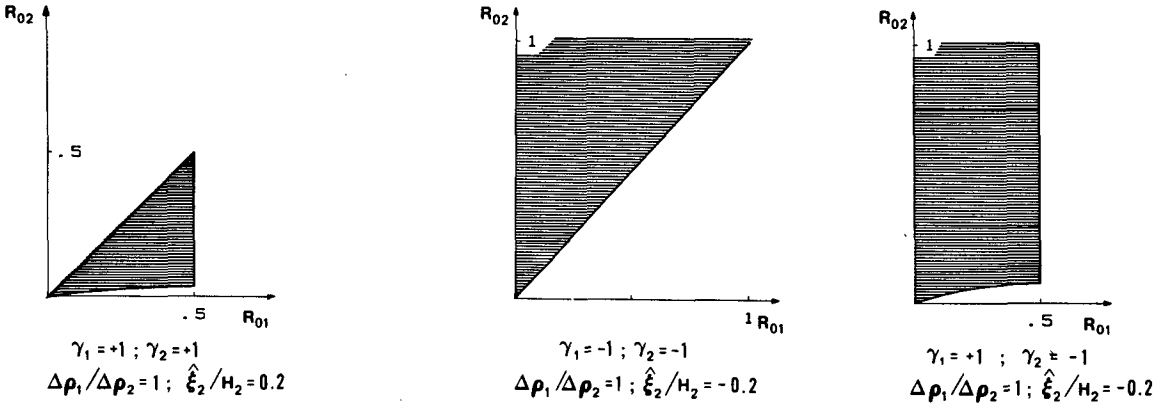

System II, linear velocity profile

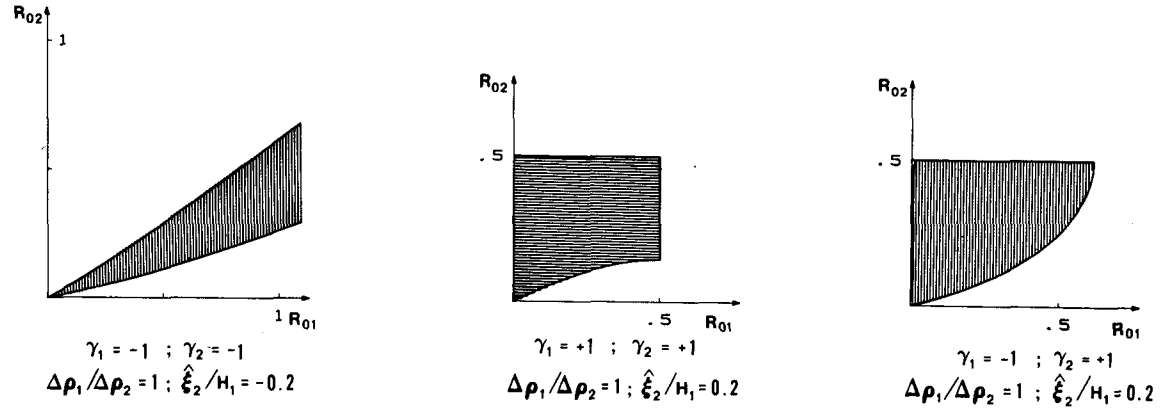

System III, linear velocity profile

FIG. 13. The permissible range for the Rossby numbers (shaded areas). The upper and lower bounds result from (i) the fact that the negative relative vorticity must be smaller than f_0 so that the eddies are inertially stable and, (ii) the conditions that $h_1 \geq 0$ and $h_2 \geq 0$ everywhere. Note that, in addition to these limitations, our scaling is valid only when the eddy length scale is at least of the order of the deformation radius.

and a column on top of it could represent a realistic situation for various vortices.

b. Limitations and weaknesses

The most important weakness of all of our systems (i.e., I, II and III) is that we have not found the *complete* first-order solution so that, in fact, we have not really proven that our solution is correct. That is to say, the complete first-order solution may involve compatibility conditions which could, perhaps, be more restrictive than our scalings. While this is no doubt a weakness, it is very difficult—and probably impossible—to overcome because it is not clear that the most general first-order solution can ever be found analytically.

An additional limitation stems from the fact that we have neglected the motion in the third layer. To illustrate the difficulty with this point we shall first look at systems II and III because, it turns out that, from this point of view, they are simpler than case I. Recently, Flierl *et al.* (1983) demonstrated that if the eddies in a stratified system are isolated in all layers (i.e., away from the eddy all the disturbances decay at a sufficiently fast rate) then the integrated sum of all the stream functions should vanish. Furthermore, Flierl (1984b) has shown that when this integral constraint is applied to a single isolated lens embedded in a layer whose depth is H, one finds that only a subset of the results agrees with the Nof (1981) assumption of steady migration rate for $H \to \infty$.

This can be interpreted in two ways. The first possibility is that the Nof (1981) basic lens model is singular (i.e., the actual solution for a finite lower layer does not reduce to a lower layer with zero velocity when $H \to \infty$). The second is that the flow in the lower layer is not necessarily isolated (i.e., the disturbances generated by the moving lens do not decay sufficiently fast for the integrated constraint to be valid). This essentially means that the isolation requirement (in the lower layer) overrestricts the system. The second possibility is more natural and, indeed, when the isolation constraint is relaxed and wave radiation is allowed, one finds that the solution for a lens with a finite lower layer (Flierl, 1984a) reduces to the Nof (1981) solution when $H \to \infty$. One, therefore, concludes that the Nof (1981) solution is not singular and that whenever the lower layer is finite there will be wave radiation. The main effect of this radiation is to alter the direction of migration. Specifically, as a result of a finite lower layer, isolated lenses move toward the southwest instead of moving straight toward the west (Flierl, 1984a).

It is expected that similar behavior will be present in system II and III. Namely, if one were to develop a model with the lower third layer being finite and active (instead of infinite and motionless) then there will probably be some modifications to the direction of migration (i.e., the joint eddies would move toward the northeast, southeast, southwest and northwest). Before proceeding, it is worth mentioning that the assumption of a motionless lower layer is valid even if the transport in that layer is of the same order as that of the other layers because the only condition that must hold is that the *velocity* is negligible.

We shall now turn our attention to the neglect of motion in the upper layer of system I. Recently, M. E. Stern has developed a topographic constraint analogous to the beta constraint discussed by Flierl *et al.* (1983) (e.g., see Mory, 1983; Nof, 1984). For a two-layer system one finds that, in a similar fashion to the β constraint, when no wave radiation is allowed in the layer surrounding the lens, the integrated sum of the pressure deviations must vanish. Unfortunately, an analysis equivalent to that performed by Flierl (1984a,b) for upper ocean eddies has not been made yet for deep ocean eddies so that we cannot say what the features of a solution with wave radiation would be like. It is expected, however, that it will not be fundamentally different from that of the upper ocean. Namely, we expect that when the upper layer is finite and active, the migration of the system will generate waves on top and these will, in turn, alter the direction of migration (through their wave drag effect).

9. Summary

This article introduces new combinations of eddies and nonlinear coupling between vortices; it focuses on topographically and β induced drifts. Solutions have been constructed under the assumptions that: (i) the ocean can be approximated by three layers, one of which can be taken to be at rest; (ii) the motion is approximately steady, frictionless and non-diffusive; and (iii) the joint eddies translate without significant changes in their structure. Three different kinds of joint vortices are considered and their behavior is given in Table 1. It can be summarized as follows:

- *Joint vortices consisting of a heavy lens situated over a sloping bottom underneath a cyclonic or anticyclonic vortex which is overlayed by an infinitely deep fluid (system I):* This system translates with shallow water on its right (i.e., "westward") or with shallow water on its left (i.e., "eastward"). Eastward drifts occur even though each individual vortex translates westward in the absence of its conjugate vortex. Both the eastward and westward speeds are unbounded but our perturbation scheme breaks down whenever the drift becomes comparable to the orbital speed.
- *Joint vortices consisting of a light lens situated above a cyclonic vortex which overlies an infinitely deep fluid (system II):* In a similar fashion to system I, both westward and eastward drifts are possible. For

westward drifts, the migration speed is of the order of the long wave speed (based on the undisturbed environmental depth); it is faster than the long wave speed whenever the lower vortex is anticyclonic. Eastward drifts are *not* bounded and are not limited to the long wave speed.

• *Joint vortices consisting of an intermediate lens which overlies an infinitely deep fluid and is situated underneath a cyclonic or anticyclonic vortex (system III):* In a similar fashion to systems I and II, eastward movements are also possible. This can occur whenever the upper vortex is cyclonic and the lower is a biconvex lens. *Both eastward and westward drifts are not limited to the long wave speed;* they are unbounded.

• *Joint vortices consisting of an intermediate lens carrying a Taylor column on top of it.* This is a special case of system III; the feature migrates toward the west at a speed which is slower than the long-wave speed. It is also slower than the speed that the intermediate biconvex lens would have if it were "sandwiched" by itself between two resting layers.

It is demonstrated that these peculiar migratory patterns stem from the presence of a side pressure force which we term *planetary lift.* This side pressure force acts in the north–south direction and alters the balance of forces in such a way that both eastward and westward movements are possible. It also causes the rather high westward drifts.

Several applications of the cases described are mentioned. First, it is pointed out that the eastward propagating vortices associated with system II (i.e., a biconvex lens situated on top of a weak cyclonic vortex) may be relevant to the warm-core rings observed north of the Kuroshio because the latter have been observed to move toward the northeast. Second, it is mentioned that the eastward propagating eddies associated with case III (i.e., a strong cyclonic vortex situated on top of a weak biconvex lens) could be of some relevance to the cold-core Gulf Stream rings which, on several occasions, have been observed to move eastward. Third, it is suggested that system III with a cyclonic vortex situated on top of a converging meniscus lens could be relevant to some cold-core Gulf Stream rings because it may explain the trapping of fluid under the thermocline. Finally, it is shown that a biconvex lens propagating with a Taylor column on top of it could be related to mid-depth vortices such as the "Meddy."

Acknowledgments. Computations and computer generated plots were made by S. VanGorder whose professional help as a programmer is much appreciated. I thank G. Flierl and R. Mied for helpful conversations regarding various aspects of isolated vortices. Discussions with G. Weatherly, D. Olson and W. White regarding the observational aspects of the problem were very useful. R. Mied made useful comments on an earlier version of this paper. This study was supported by the Office of Naval Research Contract N00014-82-C-0404 and by the Florida State University.

APPENDIX

Induced Drifts for Joint Vortices with Parabolic Velocity Profile

1. Joint vortices on a sloping bottom (system I)

The parabolic velocity profiles are given by,

$$v_{\theta 1} = \gamma_1 R_{01} f_0 r\left(\frac{r}{r_0} - 1\right) \tag{A1}$$

$$v_{\theta 2} = \gamma_2 R_{02} f_0 r\left(\frac{r}{r_0} - 1\right) \tag{A2}$$

where, as before, $\gamma_1 = 1, -1$; $\gamma_2 = 1, -1$ for anticyclonic and cyclonic eddies, respectively. The interface displacement ξ_2 and the depth h_1 are found from (A1)–(A2) and (4.3) to be,

$$\xi_2 = \hat{\xi}_2 + \frac{\gamma_2 R_{02} f_0^2 r^2}{g'(2\gamma_2 R_{02} - 1)} + \frac{2\gamma_2 R_{02} f_0^2 r^3}{3g' r_0(1 - 4\gamma_2 R_{02})} + \frac{R_{02}^2 f_0^2 r^4}{g' r_0^2} \tag{A3}$$

$$h_1 = \hat{h}_1 + \frac{(R_{01}^2 - R_{02}^2) f_0^2 r^4}{g'' r_0^2} + 2[\gamma_1 R_{01}(1 - 4\gamma_1 R_{01}) - \gamma_2 R_{02}(1 - 4\gamma_2 R_{02})] \times f_0^2 r^3 / 3g'' r_0 + [\gamma_1 R_{01}(2\gamma_1 R_{01} - 1) - \gamma_2 R_{02}(2\gamma_2 R_{02} - 1)] f_0^2 r^2 / g''. \tag{A4}$$

Substitution of these relationships into (3.11) shows that the migration speed is,

$$C = -\frac{g's}{f_0} - \left(\frac{g's}{f_0}\right)\left[\frac{\gamma_1 R_{01}(\gamma_1 R_{01} - 1) - \gamma_2 R_{02}(\gamma_2 R_{02} - 1)}{\gamma_2 R_{02}(\gamma_2 R_{02} - 1)}\right] \times \left\{\frac{3[\gamma_1 R_{01}(8\gamma_1 R_{01} - 7) - \gamma_2 R_{02}(8\gamma_2 R_{02} - 7)]}{[\gamma_2 R_{02}(\gamma_2 R_{02} - 1) - \gamma_1 R_{01}(\gamma_1 R_{01} - 1)]} + 30\right\} \times \left\{\frac{3(8\gamma_2 R_{02} - 7)}{(1 - \gamma_2 R_{02})} + 30\right\}^{-1}. \tag{A5}$$

2. Upper vortices consisting of a light lens overlying a cyclonic or anticyclonic vortex (system II)

With the aid of (A1), (A2), (5.12) and (5.13) we find,

$$\xi_1 = \hat{\xi}_1\Bigg\{1 - \frac{3}{\gamma_1 R_{01}(\gamma_1 R_{01} - 1) - \gamma_2 R_{02}(\gamma_2 R_{02} - 1)} \times \Bigg[[\gamma_1 R_{01}(2\gamma_1 R_{01} - 1) - \gamma_2 R_{02}(2\gamma_2 R_{02} - 1)]\frac{r^2}{r_0^2} + \frac{2}{3}[\gamma_1 R_{01}(1 - 4\gamma_1 R_{01}) - \gamma_2 R_{02}(1 - 4\gamma_2 R_{02})] \times \frac{r^3}{r_0^3} + (R_{01}^2 - R_{02}^2)\frac{r^4}{r_0^4}\Bigg]\Bigg\} \quad \text{(A6)}$$

and

$$\xi_2 = \hat{\xi}_2\Bigg\{1 - \frac{3}{\gamma_2 R_{02}(\gamma_2 R_{02} - 1)}\Bigg[\gamma_2 R_{02}(2\gamma_2 R_{02} - 1) \times \frac{r^2}{r_0^2} + \frac{2}{3}\gamma_2 R_{02}(1 - 4\gamma_2 R_{02})\frac{r^3}{r_0^3} + R_{02}^2\frac{r^4}{r_0^4}\Bigg]\Bigg\}. \quad \text{(A7)}$$

Substitution of (A1), (A2), (A6) and (A7) into the integral (5.10) gives, after some tedious algebra.

$$C \approx \frac{3\beta g''\hat{\xi}_2}{f_0^2}\Bigg\langle\left(\frac{\hat{\xi}_1}{\hat{\xi}_2}\right)\{\gamma_1 R_{01}/10 - 3(\gamma_1 R_{01} - \gamma_2 R_{02})/[\gamma_1 R_{01}(\gamma_1 R_{01} - 1) - \gamma_2 R_{02}(\gamma_2 R_{02} - 1)] \times [(R_{01}^2/36 - \gamma_1 R_{01}/42) - (R_{02}^2/36 - \gamma_2 R_{02}/42)]\} + \gamma_2 R_{02}\left\{\frac{1}{10} + \frac{H}{10\hat{\xi}_2} - \frac{\hat{\xi}_1}{10\hat{\xi}_2} - \frac{3(R_{02}^2/36 - \gamma_2 R_{02}/42)}{\gamma_2 R_{02}(\gamma_2 R_{02} - 1)}\right\}\Bigg\rangle \times \{R_{02}^2 - \gamma_2 R_{02}\}^{-1}\left\{1 - \frac{3\left(\frac{4}{15}R_{02}^2 - \frac{7}{30}\gamma_2 R_{02}\right)}{\gamma_2 R_{02}(\gamma_2 R_{02} - 1)}\right\}^{-1} \quad \text{(A8)}$$

which is the desired expression for the migration speed.

3. Upper vortices consisting of an intermediate lens situated underneath a cyclonic or anticyclonic vortex (system III):

For this case the interface displacements are found, from (A1), (A2) and the momentum equations, to be

$$\xi_1 = \hat{\xi}_1\Bigg\{1 - \frac{3}{[\gamma_1 R_{01}(\gamma_1 R_{01} - 1) - \gamma_2 R_{02}(\gamma_2 R_{02} - 1)]} \times \Bigg[[\gamma_1 R_{01}(2\gamma_1 R_{01} - 1) - \gamma_2 R_{02}(2\gamma_2 R_{02} - 1)]\frac{r^2}{r_0^2} + \frac{2}{3}[\gamma_1 R_{01}(1 - 4\gamma_1 R_{01}) - \gamma_2 R_{02}(1 - 4\gamma_2 R_{02})]\frac{r^3}{r_0^3} + (R_{01}^2 - R_{02}^2)\frac{r^4}{r_0^4}\Bigg]\Bigg\} \quad \text{(A9)}$$

and

$$\xi_2 = \hat{\xi}_2\Bigg\{1 - \frac{3}{\gamma_2 R_{02}(\gamma_2 R_{02} - 1)}\Bigg[\gamma_2 R_{02}(2\gamma_2 R_{02} - 1) \times \frac{r^2}{r_0^2} + \frac{2}{3}\gamma_2 R_{02}(1 - 4\gamma_2 R_{02})\frac{r^3}{r_0^3} + R_{02}^2\frac{r^4}{r_0^4}\Bigg]\Bigg\}. \quad \text{(A10)}$$

These relationships and (A1)–(A2) can now be substituted into (6.1). After some tedious, but straightforeward, algebra one finds,

$$C = \frac{3\beta g''\hat{\xi}_2}{f_0^2}\Bigg\{\frac{\hat{\xi}_1}{\hat{\xi}_2}\Bigg[\gamma_1 R_{01}(H_1/\hat{\xi}_1 - 1)/10 + \frac{3(\gamma_1 R_{01} - \gamma_2 R_{02})}{[\gamma_1 R_{01}(\gamma_1 R_{01} - 1) - \gamma_2 R_{02}(\gamma_2 R_{02} - 1)]} \times [(R_{01}^2/36 - \gamma_1 R_{01}/42) - (R_{02}^2/36 - \gamma_2 R_{02}/42)]\Bigg] + \gamma_2 R_{02}\Bigg[(1 + \hat{\xi}_1/\hat{\xi}_2)/10 - \frac{3}{\gamma_2 R_{02}(\gamma_2 R_{02} - 1)}(R_{02}^2/36 - \gamma_2 R_{02}/42)\Bigg]\Bigg\} \times (R_{02}^2/5 - 3\gamma_2 R_{02}/10)^{-1}. \quad \text{(A11)}$$

It is important to note that, as in the linear profile case, there are upper bounds on R_{01} and R_{02}. Conceptually, these bounds do not differ much from those of the linear case (Fig. 13) and, therefore, they are not presented.

REFERENCES

Batchelor, G. K., 1967: *An Introduction to Fluid Dynamics.* Cambridge University Press, 615 pp.

Charney, J. G., 1955: The Gulf Stream as an inertial boundary layer. *Proc. Natl. Acad. Sci.*, **41**, 731–740.

Cheney, R. E., 1977: Synoptic observations of the oceanic frontal system east of Japan. *J. Geophys. Res.*, **82**, 5459–5468.

Csanady, G. T., 1979: The birth and death of a warm core ring. *J. Geophys. Res.*, **84**, 777–780.

Davey, M. K., and P. D. Killworth 1984: Isolated waves and eddies in a shallow water model. *J. Phys. Oceanogr.*, **14**, 1047–1064.

Flierl, G. R., 1977: The application of linear quasi-geostrophic dynamics to Gulf Stream rings. *J. Phys. Oceanogr.*, **7**, 365–379.

——, 1979: A simple model of the structure of warm and cold-core rings. *J. Geophys. Res.*, **84**, 781–785.

——, 1984a: Rossby wave radiation from a strongly nonlinear warm eddy. *J. Phys. Oceanogr.*, **14**, 47–58.

——, 1984b: The structure and motion of warm core rings. *Aust. J. Mar. Freshwater Res.*, **35**, 9–23.

——, M. E. Stern and J. A. Whitehead, Jr., 1983: The physical significance of modons. *Dyn. Atmos. Oceans*, **5**, 1–41.

Hide, R., 1961: Origin of Jupiter's Great Red Spot. *Nature*, **190**, 895–896.

Hogg, N. G., 1973: On the stratified Taylor column. *J. Fluid Mech.*, **58**, 517–537.

——, and H. M. Stommel 1985: The heton, an elementary interaction between discrete baroclinic geostrophic vortices, and its implications concerning eddy heat-flow. *Proc. Roy. Soc. London*, (in press).

Huppert, T., 1975: Some remarks on the initiation of inertial Taylor columns. *J. Fluid Mech.*, **67**, 397–412.

Ichiye, H. E., 1955: On the behavior of the vortex in the polar front region. *Oceanogr. Mag.*, **7**, 115–132.

Ingersoll, A. P., 1969: Inertial Taylor columns and Jupiter's Great Red Spot. *J. Atmos. Sci.*, **26**, 744–752.

Jacobs, S. J., 1964: The Taylor column problem. *J. Fluid Mech.*, **20**, 581–591.

Kawai, H., 1972: Hydrography of the Kuroshio Extension. *Kuroshio Physical Aspects of the Japan Current*, H. Stommel and K. Yoshida, Eds., University of Washington Press, 235–352.

Killworth, P. D., 1983: On the motion of isolated lenses on a beta-plane. *J. Phys. Oceanogr.*, **13**, 368–376.

Kitano, K., 1974: A Kuroshio anticyclonic eddy. *J. Phys. Oceanogr.*, **4**, 670–672.

——, 1975: Some properties of warm eddies generated in the confluence zone of the Kuroshio and Oyashio currents. *J. Phys. Oceanogr.*, **5**, 245–252.

Lai, D. Y., and P. L. Richardson 1977: Distribution and movement of Gulf Stream rings. *J. Phys. Oceanogr.*, **7**, 670–683.

McCartney, M. S., 1975: Inertial Taylor columns on a beta plane. *J. Fluid Mech.*, **68**, 71–95.

McDowell, S. E., and H. T. Rossby 1978: Mediterranean water: An intense mesoscale eddy of the Bahamas. *Science*, **202**, 1085–1087.

McWilliams, J. C., and G. R. Flierl, 1979: On the evolution of isolated nonlinear vortices. *J. Phys. Oceanogr.*, **9**, 1115–1182.

——, ——, V. D. Larichev and G. M. Resnik 1981: Numerical studies of barotropic modons. *Dyn. Atmos. Oceans*, **5**, 219–238.

Mied, R. P., 1982: The birth and evolution of eastward propagating modons. *J. Phys. Oceanogr.*, **12**, 213–230.

——, and G. J. Lindemann 1979: The propagation and evolution of cyclonic Gulf Stream rings. *J. Phys. Oceanogr.*, **9**, 1183–1206.

Mory, M., 1983: Theory and experiment of isolated baroclinic vortices. Tech. Rep. WHOI-83-41, Woods Hole Oceanographic Institution, 114–132.

Nof, D., 1981: On the β-induced movement of isolated baroclinic eddies. *J. Phys. Oceanogr.*, **11**, 1662–1672.

——, 1982: On the movements of deep mesoscale eddies in the North Atlantic. *J. Mar. Res.*, **40**, 57–74.

——, 1983a: The translation of isolated cold eddies on a sloping bottom. *Deep-Sea Res.*, **39**, 171–182.

——, 1983b: On the migration of isolated eddies with application to Gulf Stream rings. *J. Mar. Res.*, **41**, 399–425.

——, 1984: Oscillatory drift of deep cold eddies. *Deep-Sea Res.*, **31**, 1395–1414.

Richardson, P. L., R. E. Cheney and L. A. Mantini, 1977: Tracking a Gulf Stream ring with a free driftng surface buoy. *J. Phys. Oceanogr.*, **7**, 580–590.

Ring Group, 1981: Gulf Stream cold-core rings: Their physics, chemistry, and biology. *Science*, **212**, 1091–1100.

Rossby, C. G., 1948: On displacements and intensity changes of atmospheric vortices. *J. Mar. Res.*, **7**, 175–187.

Shen, C. Y., 1981: On the dynamics of a solitary vortex. *Dyn. Atmos. Oceans*, **5**, 239–267.

Stern, M. E., 1975: Minimal properties of planetary eddies. *J. Mar. Res.*, **33**, 1–13.

Taylor, G. I., 1922: The motion of a sphere in a rotating liquid. *Proc Roy. Soc. London*, **102**, 180–189.

——, 1923: Experiments on the motion of solid bodies in rotating fluids. *Proc. Roy. Soc. London*, **104**, 213–219.

Tomosada, A., 1978: Oceanographical characteristics of a warm eddy detached from the Kuroshio east of Honshu, Japan. *Bull. Tokai Reg. Fish. Res. Lab.*, **94**, 59–103.

Warren, B. A., 1967: Notes on translatory movement of rings of current with application to Gulf Stream eddies. *Deep-Sea Res.*, **14**, 505–524.